UNIVERSITY OF BIRMINGHAM

Polymer-Supported 1-(4-vinylbenzyl)-[4,4'-bipyridin]-1-ium Chloride Ligand for Pd(II) Complexation

by

Adrián Pérez López

A thesis submitted to the University of Birmingham

for the degree of Master of Science by Research

School of Chemistry

College of Engineering and Physical Sciences

University of Birmingham

February 2019

Abstract

The synthesis of metal containing nanoparticles have been widely studied during the last decades. These compounds display properties that can be easily varied to adapt to finely selected conditions. This makes them suitable for applications such as catalysis and medicine.

The goal of this project is the synthesis of a water-soluble polymer made of a one-step synthetic bipyridine-derivative monomer as well as the study of its ability to interact with palladium(II) salts to form particles.

For this, the optimization of the synthesis of the monomer 1-(4-vinylbenzyl)-[4,4'-bipyridin]-1-ium chloride has been developed. This monomer has been polymerized together with acrylamide in order to enhance the water solubility of the final polymer.

The Kelen-Tüdos method has been performed in order to investigate the polymer conformation. The resultant polymer has been characterized using techniques such as GPC, ^{1}H NMR and DLS.

Finally, the interaction between the copolymer and a precursor palladium complex has been studied. For this, UV-Vis and ^{1}H NMR experiments have been performed in order to study the interactions between monomer and palladium centers as well as polymer palladium. In addition, DLS has been used to study the effect of the addition of the metal to a polymer solution in the particles size.

Acknowledgements

Firstly, I would like to express my sincere gratitude to my supervisor, Dr Francisco Fernández-Trillo, for his patience guidance and supervision. This dissertation would not be possible without his academic and personal support. I am grateful for having the opportunity to work under his supervision.

Thanks to my colleagues that I spent one full year with. It was nice to know you all. Andy, Oliver, Manal, Krystian, Pavan, Carlos, Charlotte, Tom and Laim thanks so much for the time we spent in and out of the lab and for the fantastic international meals. Special thanks to Adam for his personal and scientific support. I really enjoyed our breaks and after works.

I would like to thanks the Spanish crew. Jordi, Manolo, María, Sara, Xavi and Pilar. This experience would not be the same without you. Thank you for welcoming me and make my time in Birmingham easier and funnier.

Special thanks to Zelu. The person who I shared most of the time during this experience. Many things to remember. All of them great. I hope to see the "tortuguita" again.

Thanks to the person who made me feel as I was at home: Mariquilla. Thank you so much for the intense conversations we had. Thank you for the laughs and the support. Thank you for everything.

I would like to thank my parents for supporting me during my educational years. My father who always trusted in me and encouraged me to continue my education. My mother for her endless love support.

Finally, thanks to all the technicians in the School of Chemistry who have contributed to this theses (Chi, Peter, Allen and Cécile).

To all of you thanks.

Contents

List of Figures

List of Tables

Abbreviations

℃	Degree centigrade
δ	Chemical shift
µL	Microliter
AcOEt	Ethyl acetate
ACVA	4,4′-Azobis(4-cyanopentanoic acid)
AEMA	2-(acetoacetoxy)ethyl methacrylate
COSY	Correlation spectroscopy
CTA	Control transfer agent
d	Doublet
DEPT	Distorsion enhancement by polarization transfer
DLS	Dynamic Light Scattering
DMSO	Dimethyl sulfoxide
DP	Degree of polymerization
FRP	Free Radical Polymerization
g	Grams
kD	Kilodalton
mg	Miligrams

MMA	Methyl methacrylate
NP’s	Nanoparticles
GPC	Gel permeation chromatography
HMBC	Heteronuclear multiple-bond correlation spectroscopy
HPLC	High performance liquid chromatography
HSQC	Heteronuclear single-quantum correlation spectroscopy
m	Multiplet
MCV	Method of continuous variations
MHz	Megaherz
MS	Mass spectrometry
Mw	Molecular weight
m/z	Mass/charge ratio
NMR	Nuclear magnetic resonance
Pd	Palladium
ppm	Parts per million
s	Singlet
T	Temperature
THF	Tetrahydrofuran
t	Time

UV-Vis	Ultraviolet-visible

Chapter 1

Introduction

Over the last two decades, the study of C-C cross-coupling reactions has become a hot-topic in synthetic chemistry.[1] However, the recently acquired commitment to the development of environmental friendly chemistry has driven the study of new synthetic conditions to address environmental issues. The substitution of toxic and harmful solvents to prioritize the usage of water-based systems have considerable advantages not only due to its non-toxic and non-flammable features, but also due to economic reasons.[2] Moreover, it has been found that the dielectric constant of the water is an advantage in reactions that results in insoluble products, leading to cleaner and faster reactions.[3] Therefore, the study of new catalytic-systems in water shows up as an essential step to achieve efficient and environmentally sustainable synthetic conditions.

In this context, the preparation of polymer-supported functional ligands and palladium complexes has been studied during the last few years showing as good catalytic activity in C-C cross-coupling reactions as using monomeric complexes.[4] In particular, polymers-supporting pyridine-based ligands have shown good catalytic activity due to their capability to lower the transition state energy of C(sp^3)-H activation.[5] Nevertheless, there are few of these polymer nanoparticles that are stable due to the lability of Pd-pyridine binding.[6] Some phosphine-based ligands have been studied showing great binding features and high catalytic activity.[7] However, the harsh conditions required in C-C cross-coupling reactions result in the oxidation of phosphine ligands leading in the loss of catalytic activity,[8] which makes pyridine derivatives more suitable ligands.[9] On the other hand, heterogeneous systems have been mostly used in

order to facilitate the recovery of the catalyst.[10] However, it has been shown that homogeneous systems displays some advantages such as higher selectivity, softer temperature and higher catalytic activity.

Previous work on polymer NP's made of metal-crosslinked polymers has been done recently with different metals and polymers. Christopher Barner-Kowollik et al. reported the synthesis of platinum[11] and palladium[12] polymers NP's made of a copolymer based in styrene together with triarylphospine moieties as functional group along the backbone (Figure 1). The catalytic activity of both complex was studied. In the case of polymer containing platinum(II) salts, the catalytic activity was successfully demonstrated using as example the amination of allyl alcohols. In addition, the recovery of the catalyst was achieved. In the case of complex made of palladium (II), Sonogashira C- C coupling reactions were performed and results showed good catalytic activity.

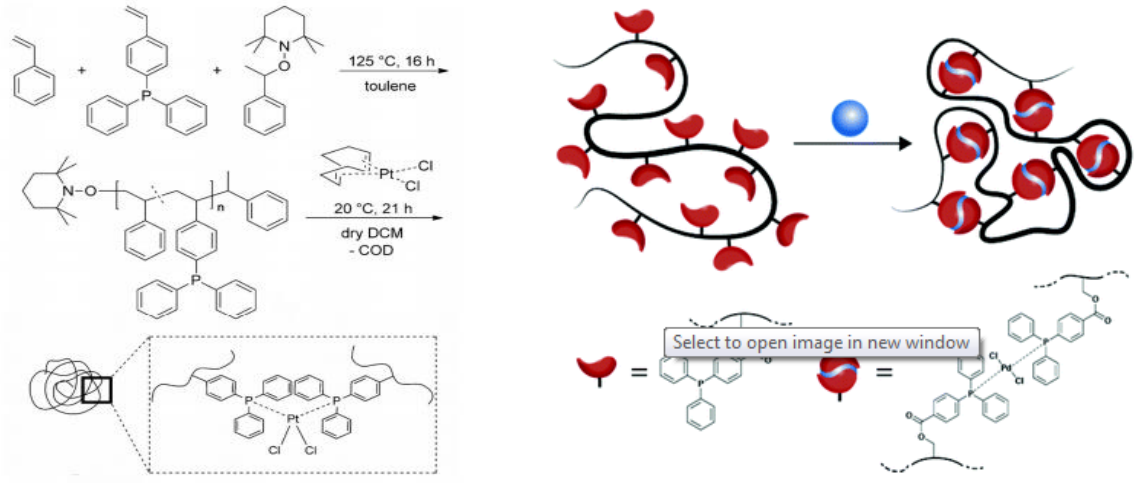

Figure 1. Polymer NP´s of palladium and platinum containing reported by Christopher Barner-Kowollik et al.

N. Gabriel Lemcoff et al. reported the obtaining of 1,4-polybutadieneand rhodium complex as shown in figure 2.[13] In this case the functional groups that binds the metal are vinyls located along the backbone of the polymer chain.

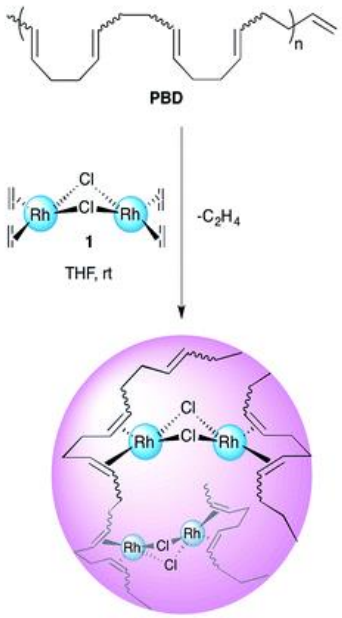

Figure 2. Polymer NP's of ruthenium containing reported by N. Gabriel Lemcoff et al.

Jose A. Pomposo et al. reported the preparation of copper containing nanoparticles attached to a copolymer of MMA and AEMA. It was demonstrated the high catalytic activity of these NP's for the oxidative coupling of terminal alkynes (Figure 3).[14]

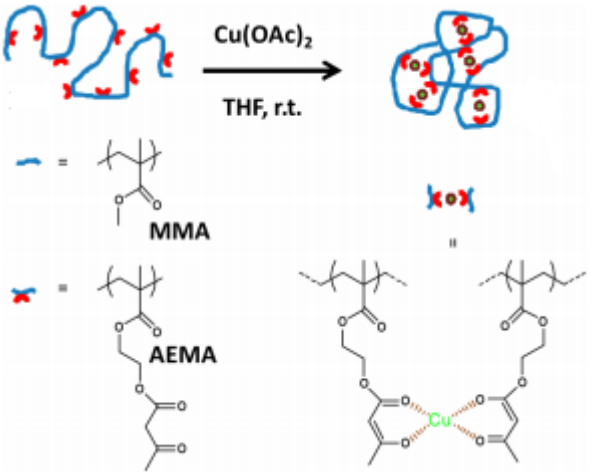

Figure 3. Polymer NP's of copper reported by Jose A. Pomposo et al.

All the examples presented above showed different polymers cross-linked by different metals that formed NP's successfully. In addition, all of them presented good catalytic activity for different applications. Nevertheless, these compounds are only soluble in organic solvents. In this work, we aimed the formation of water soluble polymer NP's for potential applications as

catalyst in C-C cross-coupling reactions in water.

1.1- Challenges in the synthesis of copolymers

It is well known that, in two component polymeric systems, the different chemical properties of the monomers affect their reactivity and therefore, the distribution of the monomers along the polymer chain. According to this, linear polymers can be divided in three main groups.[15] Random polymers, where monomer are distributed randomly along the polymer chain. Gradient polymers, which show a gradual variation in the composition long the polymer chain. Finally block copolymers which are defined as a polymer comprising molecules in which there is a linear arrangement of blocks, a block being defined as a portion of a polymer molecule in which the monomeric units have at least one constitutional or configurational feature absent from the adjacent portions.

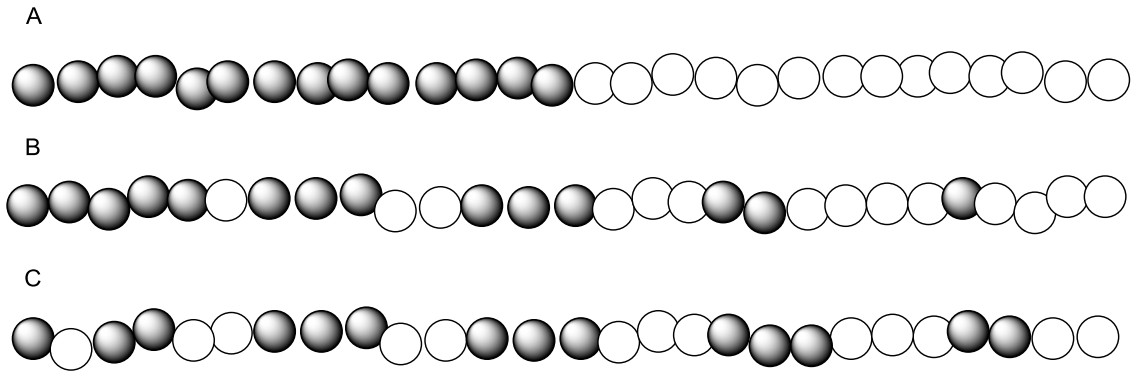

Figure 4. Representation of the three different arrangements of a linear polymer. (A) Block copolymer. (B) Gradient copolymer. (C) Random copolymer.

With this in mind, it is essential to perform kinetic studies to determine the reactivity ratio of the monomers in order to have a better insight of the polymer conformation.

There are a few different models to determine the polymer composition by obtaining the monomer reactivity ratios.[16] In this work, we will only focus on those based on the terminal model since it is presented as the best for conformation predicting. First, Mayo and Lewis put forwarded their method which equation is as follow.[17]

$$\frac{dM_1}{dM_2} = \frac{r_1 M_1^2 + M_1 M_2}{r_2 M_2^2 + M_1 M_2} \quad (1)$$

This method allows for the calculation of the reactivity ratios $\mathbf{r_1}$ and $\mathbf{r_2}$ of a pair of monomers based on the molar concentration of each one of the monomers in the feed $\mathbf{M_1}$ and $\mathbf{M_2}$, and the molar concentration in the final polymer $\mathbf{m_1}$ and $\mathbf{m_2}$.

On the other hand, Fineman and Ross developed a linear graphical method.[18] Being $y = (m_1/m_2)$ and $x = (M_1/M_2)$ the molar ratios of the monomers in the copolymer and in the feed respectively, the equation (1) can be rearranged as follow:

$$\frac{x(1-y)}{y} = r_2 - \frac{x^2}{y} r_1 \quad (2)$$

When the equation (2) is simplified as G=x(1-y)/y and F=x^2/y the equation (3) is obtained:

$$G = r_1 H - r_2 \quad (3)$$

Finally, by plotting G as ordinate and H as abscissa, a straight line is obtained with slope $\mathbf{r_1}$ and intercept $-\mathbf{r_2}$. It is important to take into account that this method is only accurate when the conversion of the monomers is below 10%. Above this percentage of conversion, the since it focuses on the concentrations of all the active chains terminating. Therefore, this concentration is calculated using the steady state approximation. This condition is only fulfilled at the very beginning of the polymerization.

Kelen and Tüdos improved the method by adding an arbitrary constant α in the Fineman-Ross equation. The final equation after the addition of the new constant is as follow:[19]

$$\eta = \left(r_1 + \frac{r_2}{\alpha}\right)\xi - \frac{r_2}{\alpha} \quad (4)$$

where;

$$\eta = \frac{G}{\alpha + F}; \qquad \xi = \frac{F}{\alpha + F} \qquad (5)$$

Where $\alpha = \sqrt{F_m x F_M}$ is a constant composed by F_M which is the highest value of F whereas F_m is the lower, both calculated experimentally. Finally, by plotting η vs ξ according the equation (1), a straight line is obtained. Finally, $\mathbf{r_1}$ and $\mathbf{r_2}$ are calculated by using the least-squares technique.

The KT method improved the FR in the way that reactivity ratios can be calculated not only at low conversions, but also at high conversions by using the partial conversions of the monomers. It is important to mention that the reactivity ratios of the monomers obtained by the application of the KT method are not absolute. This means that the value of the reactivity of a certain monomer depends on the monomers in the system.

The reactivity ratios indicate the preference of each one of the monomers to react with itself or with the other monomer in the system:

- $r_1 < 1$ → Monomer 1 reacts preferable with monomer 2 than with itself.
- $r_1 \approx 1$ → Monomer 1 reacts with itself and with monomer 2 in the same way.
- $r_1 > 1$ → Monomer 1 reacts preferable with itself than with monomer 2.

Figure 5 shows different compositions of a hypothetical polymer when varying one of the reactivity ratios. Figure 6 shows the composition of a polymer when both reactivity ratios are the same.

For instance, for a system formed by monomer 1 and monomer 2:

- $r_1 \approx r_2 >> 1$ → in the case in which both reactivity ratios are much higher than 1, the two monomers only react with themselves and not with each other. This leads to a mixture of two homopolymers.
- $r_1 \approx r_2 > 1$ → when both reactivity ratios are higher than 1, homopolymerization of each monomer is favoured. Nevertheless, in the event of cross polymerization, the chain-end will continue to add the new monomer and form a block copolymer.

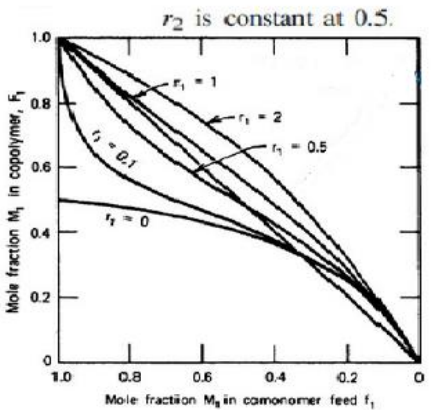

Figure 5. Theoretical compositions of a polymer when monomer reactivity ratio of monomer 2 is fixed at 0.5 and varying the monomer feed at different reactivity ratio of monomer 1.

- $r_1 \approx r_2 \approx 1$ → when both reactivity ratios are close to 1, a statistical or random copolymer is formed.
- $r_1 \approx r_2 \approx 0$ → in the case of both values of reactivity tend to 0, the monomers are unable to homopolymerize leading in a random copolymer.

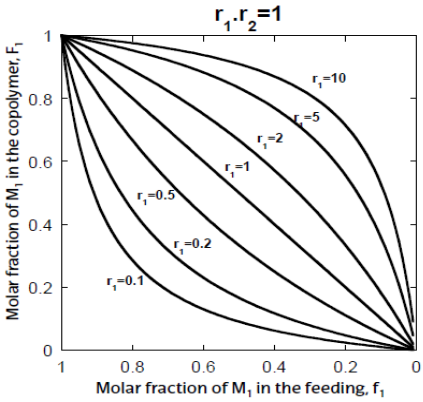

Figure 6. Theoretical composition of a copolymer when both reactivity ratios are equal but changing the polymer feed.

- $r_1 >> 1 >> r_2$ → in the initial stage of the copolymerization, monomer 1 is incorporated faster and the copolymer is rich in monomer 1. When this monomer get consumed, more monomer 2 segments are added. This is called composition drift.
- $r_1, r_2 < 1$ → in the case that both reactivity ratios are below 1, the system has an azeotrope, where feed and copolymer composition are the same.

Having this in mind, when both monomer have reactivity ratios above 1 the system tends to form block copolymers. By contrast, when both polymers have reactivity ratios around 1, the

monomers distribute randomly along the polymer chain. Finally, when one of the monomers has reactivity ratio above 1, and the other one is below 1, the final polymer is a random polymer with a higher content of the more reactive monomer. As consequence, this difference in reactivity has a huge impact in the arrangement of the polymer and for hence it might have an effect in the performance of the polymer.

Experimentally, a set of reactions must be performed in the entire range of monomer feed ratio, from 0.1:0.9 to 0.9:0.1 (M_1:M_2) and at the same reaction conditions. The conversions are obtained via ^{1}H NMR. Once the data are collected, calculations are done as explained above and parameters are plotted.

1.2- The choice of Pd-pyridine

Palladium catalysed cross-coupling reactions have been widely studied during the last decades, specially the Suzuki-Miyaura coupling due to catalytic activity, available starting materials and catalyst toxicity.[20] Most of the palladium catalyst used are supported by electron-rich phospane[21] and N-heterocyclic carbene (NHC) ligands.[22] Nevertheless, these catalyst showed high sensitive to oxygen. Thus, these reactions must be carried out under inert atmosphere. Recently, studies on this reactions have shown that nitrogen-based chelate ligands as β-diketiminate,[23] porphyrin[24] and pyridine-based compounds[25] provide the system with rigidity and high stability. This higher stability allows perform the cross-coupling reactions under aerobic conditions.[26]

It is important to take into account that most of the pyridine-based ligands are chelates due to the fact that provide the complex with a higher stability. This effect is especially important since the lability of the complex formed. It is well known that Pd-Pyridine bonds are significantly labile leading in self-sorting processes where the resultant structure is the more stable

thermodynamically.[27] As it will be discussed later, in the case presented here, this effect is specially exacerbated due to the fact that the monomer synthetized for this work (1-(4-vinylbenzyl)-[4,4'-bipyridin]-1-ium chloride) is deficient in electronic density due to its positive charge. This results in a less efficient complex binding which leads to a more labile interaction between the monomer and the metal. Considering this and having in mind that the monomer synthesized in this work is a monodentate ligand, introducing the mentioned ligand in a polymer will enhance the stability of the particles.

With this in mind, one of the key steps in this project is the study of the ability of the bipyridine-derivative monomer studied to bind palladium(II) metal centers. Similar structures have been studied during the last 40 years, especially in the field of supramolecular chemistry in the synthesis of self-assembled coordination complex. Starting in 1990 for the simplest square structure reported by professor Fujita,[28] the synthesis of new ligands has led to structures that are more complex.[29] One of the remarkable features of these structures is the lability of the interactions between the monomer and the palladium(II) centers as mentioned above. Therefore, the combination of bipyridine-derivative ligands and palladium (II) complex provide these compounds the ability of modulate themselves depending on the conditions in a self-sorting process.

In order to characterize the complex formed by the synthetized monomer and the palladium(II) complex, the Job Plot method was performed.[30] The also called Method of Continuous Variations (MCV) provides qualitative and quantitative insights into the stoichiometry underlying association of *m* molecules of **A** and *n* molecules of **B** to form $\mathbf{A}_m\mathbf{B}_n$.

In his work, Job showed that plotting the intensity of a physical property corresponding to the complex formation versus the mole fraction of the mixtures, afforded a plot that provides

information of the stoichiometry of the complex. Any physical property that correlates linearly a physical property with the concentration of the complex can be used in this analysis: Conductivity, UV-Vis absorbance, NMR spectroscopy, etc.[31]

Experimentally, MCV holds the total molar concentration of both compounds constant and varies the relative proportions of **A** and **B**. The units on the x axis morph from concentration to mole fraction of A or B (XA or XB such that XA = [A]/{[A]+[B]} = 1-XB).

The shape of the curve gives qualitative information into the strength of the binding between components as shown in figure 7. Therefore, the more acute is the curve, the higher is the stability constant. This is because when the stability constant of a complex is high, the formation of the complex occurs as the monomer is added so the absorbance due to the complex formation will increase faster. By contrast, a gentle curvature means a balanced equilibrium. When the stability constant is low, an equilibrium is stablished between the ligand free and the ligand forming the complex. This means that part of the monomer added will be in the solution and some other forming the studied complex.

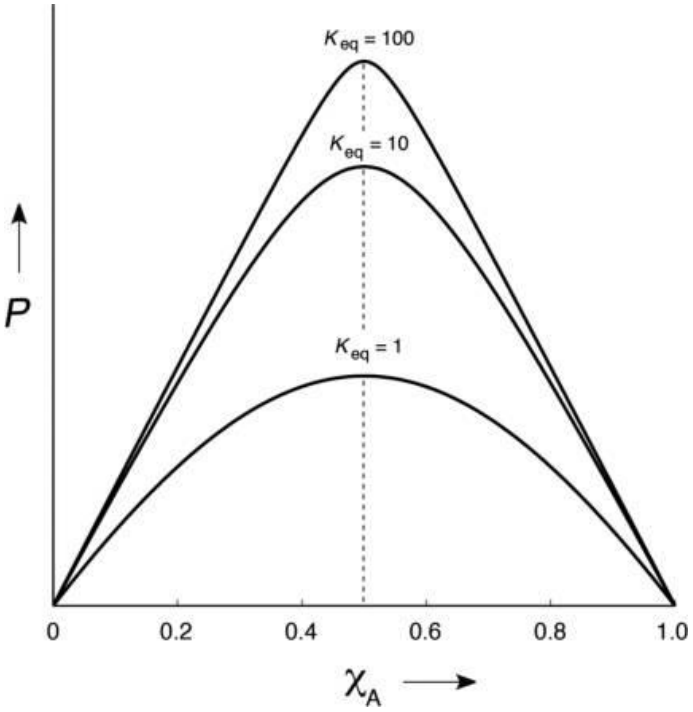

Figure 7. Job plot representation for complex with different stability constants.

In addition, although the Job analysis does not give any quantitative information on the different orders of stoichiometry *n*:*n* (1:1, 2:2…), changes in the shape of the curve can give indications on this as shown in figure 8.

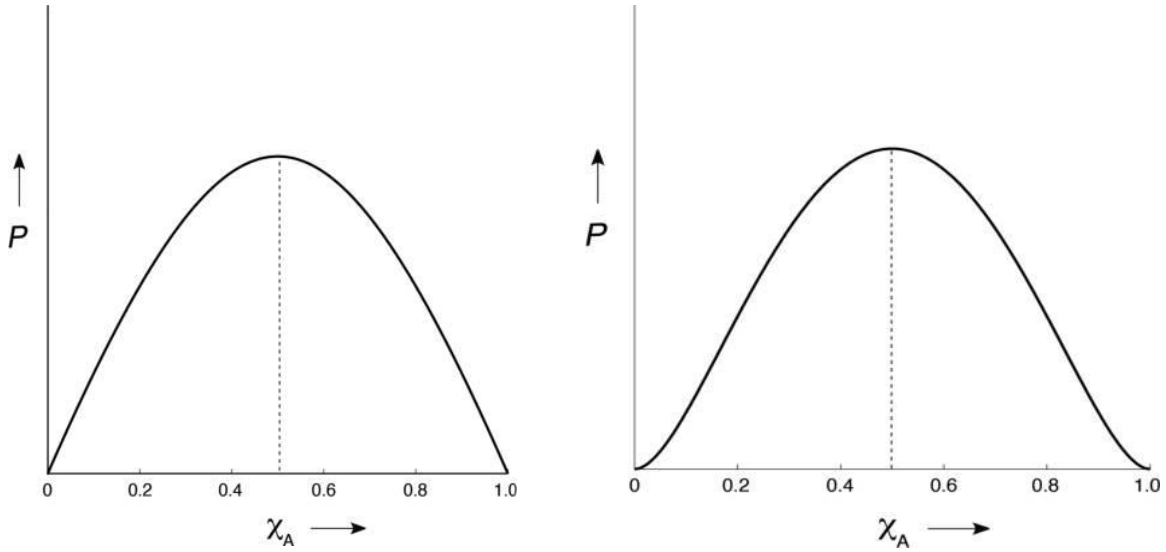

Figure 8. Left side image: Representation of a Job Plot deriving from a 1:1 complex with a maximum in $X_A = 0.5$. Right side image: Job Plot corresponding to a binary complex 2:2

Finally, the position of the maximum determines quantitatively the stoichiometry of the complex. If the position of the peak is at $X = 0.5$ it means that the stoichiometry of the complex is 1:1 as shown in the left image of figure 8. Finally, if the stoichiometry is 2:1, the maximum is located at $X = 0.33$ or $X = 0.66$ depending the component represented in the x axis as shown in figure 9.

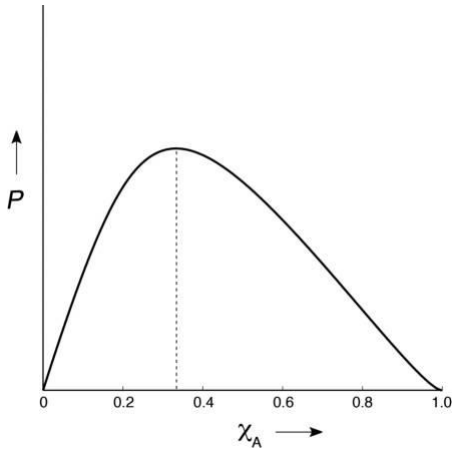

Figure 9. Representation of a Job Plot deriving from a 2:1 complex with a maximum in XA = 0.33.

Herein, we report the preparation and characterization of a water-soluble polymer-supported bipyridine-derivative ligand for Pd(II) complexation with potential applications in homogeneous C-C cross-coupling catalysis. The copolymer was made of acrylamide to enhance the water-solubility and 1-(4-vinylbenzyl)-[4,4'-bipyridin]-1-ium (Monomer **1**) chloride as monodentate water-soluble ligand able to bind palladium(II) complex.

For this, the following stages must be achieved

- Synthesis and characterization of 1-(4-vinylbenzyl)-[4,4'-bipyridin]-1-ium chloride.

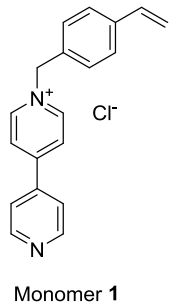

*Figure 10. Structure of the 1-(4-vinylbenzyl)-[4,4'-bipyridin]-1-ium chloride (Monomer **1**).*

- Introduce the monomer **1** into a water-soluble polymer. For this, acrylamide was used as comonomer due to its water-solubility.

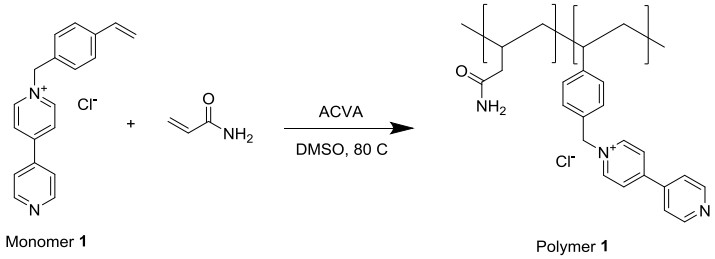

*Figure 11. Synthesis of the polymer **1**.*

- Finally, study of the interactions polymer **1**-palladium and their ability to form nanoparticles.

Chapter 2

Experimental section

2.1- General methods

All chemicals and solvents were purchased from Sigma-Aldrich®, Fisher Scientific®, VWR® or Acros®, and used without further purification. Dynamic light scattering (DLS) was carried out in a Zetasizer Nano ZSP (Malvern Instruments Ltd.) stabilised at 25 °C. DLS was read at 173° (backscattering) for 30 seconds in triplicate. The refractive index parameter of the acrylamide was set at 0.170. Nuclear Magnetic Resonance (NMR) spectra were recorded on either a Bruker Avance III 300 MHz or a Bruker Avance III 400 MHz spectrometer. Chemical shifts are reported in ppm (units) referenced to the following solvent signals: dimethylsulfoxide (DMSO)-d_6 H 2.50 ppm and D_2O H 4.79 ppm. All conversions were obtained via ^{1}H NMR using syringic acid as a reference. Gel Permeation Chromatography (GPC) was performed with a Shimadzu Prominence LC-20A fitted with a Thermo Fisher Refractomax 521 Detector. Molecular weights were calculated based on a standard calibration method using a Polyethylene glycol (PEG) kit. The polymers were analysed using a Phosphate Buffered Saline 0.0095 M (PO_4^{3-}) without Ca and Mg as the eluent and a flow rate of 1 mL min^{-1}. The instrument was fitted with a precolumn and two Agilent PL aquagel-OH column (300 × 7.5 mm, 8 mm) and run at 35 °C.

Dialysis was carried out in deionised water at room temperature for a minimum of 72 hours using a Spectra/Por 6 1 kD Molecular weight cut-off (MWCO) 38 mm width membrane.

2.2- Synthesis of 1-(4-vinylbenzyl)-[4,4'-bipyridin]-1-ium chloride

In a typical experiment, an excess of 4,4'-bipyridine (5.0 g, 31.9 mmol) was dissolved in toluene (50.0 mL). 4-vinylbenzyl chloride (1.0 mL, 6.4 mmol) was added and the crude was stirred at reflux overnight to obtain 1-(4-vinylbenzyl)-[4,4'-bipyridin]-1-ium chloride (monomer **1**). The final product which was not soluble in toluene was filtered and washed with the same solvent to get rid of the excess of 4,4'-bipyridine to yield 61% of a red solid.

^{1}H NMR (300 MHz, D_2O) δ (ppm): δ 9.01 (d, *J* = 7.0 Hz, 2H), 8.77 (d, *J* = 6.3 Hz, 2H), 8.40 (d, *J* = 6.9 Hz, 2H), 7.90 (d, *J* = 6.3 Hz, 2H), 7.54 (dd, *J* = 36.9, 8.3 Hz, 4H), 6.82 (dd, *J* = 17.7, 10.9 Hz, 1H), 5.91 (d, *J* = 17.7 Hz, 1H), 5.87 (d, *J* = 8.3 Hz, 1H), 5.38 (d, *J* = 11.0 Hz, 1H).

^{13}C NMR (400 MHz, DMSO) δ 153.22, 151.43, 145.75, 141.33, 138.65, 136.27, 134.13, 129.71, 127.33, 126.34, 122.44, 116.22, 63.13.

TOF MS: m/z 273.1.

2.3- Synthesis of poly-(acrylamide-co-(1-(4-vinylbenzyl)-[4,4'-bipyridin]-1-ium chloride))

In a typical experiment 1-(4-vinylbenzyl)-[4,4'-bipyridin]-1-ium chloride (200.0 mg, 0.62 mmol), acrylamide (398.0 mg, 5.54 mmol), 4,4′-Azobis(4-cyanopentanoic acid) (88.9 mg, 0.31 mmol) were dissolved in DMSO (15.4 mL). At this stage, 100 µL of the crude were taken to aid in the calculation of the conversion. Then, the reaction mixture was sealed and degassed with argon for 30 min. After degassing, the reaction mixture was heated at 80 ºC for 120 min. After the polymerisation, a 100 µL aliquot of the crude was taken in order to calculate the conversion. The conversions were calculated via ^{1}H NMR using syringic acid as reference. The resultant red solution was dialysed against water. The water was finally removed by lyophilisation to yield a red powder.

In the case of kinetic experiments, aliquots were transferred from the degassed flask to different sealed vials through a cannula. Every vial was further degassed for 15 min. The reaction was quenched by oxygen once the septum was taken off. ^{1}H-NMR (300 MHz, D2O) δ (ppm): δ 8.90 (s, 2H), 8.60 (s, 2H), 8.29 (s, 2H), 7.75 (s, 2H), 7.33 (s, 4H), 5.74 (s, 1H), 2.43 – 0.67 (m, 32H).

GPC: M_w = 7236 g mol^{-1} Đ = 3.3.

2.4- Study of interactions between the precursor Pd(II) complex and 1-(4-vinylbenzyl)-[4,4'-bipyridin]-1-ium chloride

The palladium salt used in this study was the bis(acetonitrile)dichloropalladium(II). Experimentally, all solutions prepared for the study of the interaction Pd(II)-Monomer were prepared at room temperature either in deionized water for UV-Vis and DLS or D_2O for ^{1}H NMR analysis and stirred for a minimum of 1 hour. The calculations for the preparation of the mixtures palladium/polymer were made based in the stoichiometry between the precursor palladium salt with respect to the amount of monomer along the polymer chain, taking into account the conversion of each one of the monomers.

Three analytical techniques were used to study the interactions between metal centres and the monomer **1**. DLS was performed in order to find out whether the addition of the palladium salt to a polymer solution either induces the formation of particles or provokes a change in the size of the particles already formed. In addition, ^{1}H NMR spectroscopy and UV-Vis spectrometry was performed to obtain quantitative data for the study of the complexation of the precursor palladium complex by the monomer **1** and the polymer **1**.

2.4.1 Sample preparation for the study of the interactions monomer-palladium in UV-Vis

For the experiments performed in this part of the project, different concentration monomer solutions with different ratios monomer-palladium complex were prepared. Experimentally,

one standard solution of monomer 1 and one standard solution of the precursor palladium complex were prepared. Then, the solutions were mixed as indicated in table 1:

Solution A→ 5.0 mg of monomer **1** in 25.0 mL of water.

Solution B→ 3.48 mg of bis(acetonitrile)dichloropalladium(II) in 5.0 mL of water.

Table 1. Preparation of samples for the study of the interactions monomer 1-palladium via UV-Vis analysis.

eq of palladium	Water (mL)	Solution A (mL)	Solution B (µL)	Total volume (mL)
0.0	0.500	0.500	0	1.000
0.1	0.498	0.500	2	1.000
0.3	0.494	0.500	6	1.000
0.5	0.490	0.500	10	1.000
0.7	0.486	0.500	14	1.000
1.0	0.480	0.500	20	1.000

The protocol for preparing the samples was as follow; First, the volumes of water and **solution A** presented in table 1 were transferred to a vial so when the palladium salt solution was added the concentration of the monomer was the same for all the samples. Then, the **solution B** was added. Finally, all samples were stirrer for 1 hour and then diluted 1 in 10.

On the other hand, for the Job Plot analysis, two standard solutions were prepared:

Solution C→ 1.0 mg of monomer **1** in 50.0 mL of water.

Solution D→ 0.8 mg of bis(acetonitrile)dichloropalladium(II) in 50.0 mL of water.

Then, **solutions C** and **D** were mixed as shown in table 2.

Table 2. Preparation of samples for the Job Plot analysis.

X_{M1}	Solution A (mL)	Solution B (mL)
0.1	0.1	0.9
0.2	0.2	0.8
0.3	0.3	0.7
0.4	0.4	0.6
0.5	0.5	0.5
0.6	0.6	0.4
0.7	0.7	0.3
0.8	0.8	0.2
0.9	0.9	0.1

Samples were stirred for 1 hour before the UV-Vis analysis.

2.4.2 Sample preparation for the study of the interactions monomer-palladium via ^{1}H NMR

The samples for the study of the interactions monomer-palladium via ^{1}H NMR were prepared in D_2O and adding DMSO as reference for the quantification of the signals. Two standard solutions were prepared as follow:

Solution E→ 1.8 mg of monomer **1** in 5.0 mL of D_2O.

Solution F→ 1.4 mg of bis(acetonitrile)dichloropalladium(II) in 5.0 mL of D_2O.

Samples were prepared as indicated in table 3.

Table 3. Preparation of samples for Job Plot via ^{1}H NMR.

X_{M1}	Solution E (mL)	Solution F (mL)	DMSO (µL)
0.1	0.1	0.9	2.0
0.2	0.2	0.8	2.0
0.3	0.3	0.7	2.0
0.4	0.4	0.6	2.0
0.5	0.5	0.5	2.0
0.6	0.6	0.4	2.0
0.7	0.7	0.3	2.0
0.8	0.8	0.2	2.0
0.9	0.9	0.1	2.0

All the samples were stirred one hour before the analysis.

2.4.3 Sample preparation for the study of the interactions polymer-palladium in ^{1}H NMR

For the qualitative study of interaction polymer-Pd, a standard solution of polymer and a bis(acetonitrile)dichloropalladium(II) were prepared as follow:

Solution G→ 6.7 mg of polymer 1 in 2.0 mL of D_2O.

Solution H→ 0.6 mg of bis(acetonitrile)dichloropalladium(II) in 1.0 mL of D_2O.

Then, the standard solutions were mixed as shown in table 4.

Table 4. Preparation of the samples for the qualitative study of the interactions between the precursor complex and the polymer.

eq of palladium	Soluiton G (µL)	Solution H (µL)	D_2O (µL)
0.0	300	0	300
0.3	300	54	246
0.5	300	90	210
1.0	300	181	119
1.5	300	271	29
2.0	300	300	0

2.4.4 Sample preparation for the study of the interactions polymer-palladium in DLS

The DLS experiments were performed at three different concentrations of polymer **1**. The samples were prepared as follow:

<u>0.5 mg mL^{-1} final concentration of polymer 1 in the samples</u>

Solution I→ 10.0 mg of polymer 1 in 10.0 mL of H_2O.

Solution J→ 0.8 mg of bis(acetonitrile)dichloropalladium(II) in 10.0 mL of H_2O.

<u>1.0 mg mL^{-1} final concentration of polymer 1 in the samples</u>

Solution k 20.0 mg of polymer 1 in 10.0 mL of H_2O.

Solution L→ 1.8 mg of bis(acetonitrile)dichloropalladium(II) in 10.0 mL of H_2O.

2.0 mg mL^{-1} final concentration of polymer 1 in the samples

Solution M→ 40.0 mg of polymer 1 in 10.0 mL of H_2O.

Solution N→ 3.6 mg of bis(acetonitrile)dichloropalladium(II) in 10.0 mL of H_2O.

The standard solutions were mixed as shown in table 5.

Table 5. Sample preparation for DLS analysis.

eq of palladium	Water (µL)	Solutions I K M (µL)	Solutions J L N (µL)	Total volume (mL)
0.0	750	750	0	1.5
0.1	675	750	75	1.5
0.3	525	750	225	1.5
0.5	375	750	375	1.5
0.8	150	750	600	1.5
1.0	0	750	750	1.5

All the samples were filtered using 45.0 µm nylon filter tips and stirred for 1 hour before the measurements.

Chapter 3

Synthesis and characterization of 1-(4-vinylbenzyl)-[4,4'-bipyridin]-1-ium Chloride

Monomer **1** was prepared by reacting an excess of 4,4'-bipyridine with 4-vinylbenzyl chloride in toluene under reflux for 24 h to afford an average yield of 61% (Figure 12). Since monomer **1** was not soluble in toluene, the excess of 4,4'-bipyridine could be removed by washing with the solvent.

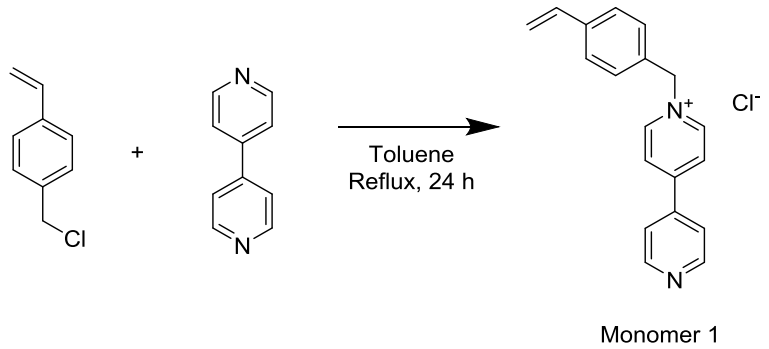

Figure 12. Scheme of 1-(4-vinylbenzyl)-[4,4'-bipyridin]-1-ium chloride synthesis.

^{1}H NMR (Figure 13) and mass spectrometry (Figure 14) were performed to characterize the product obtained.

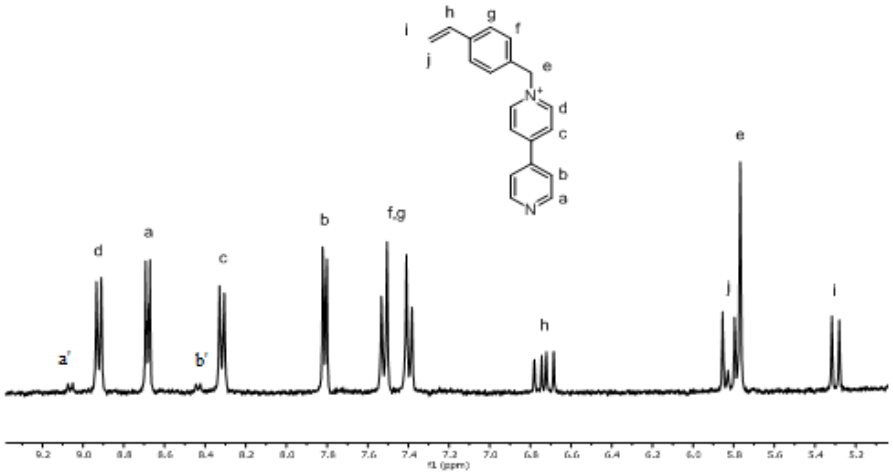

*Figure 13. ^{1}H NMR of the product **1** in D_2O.*

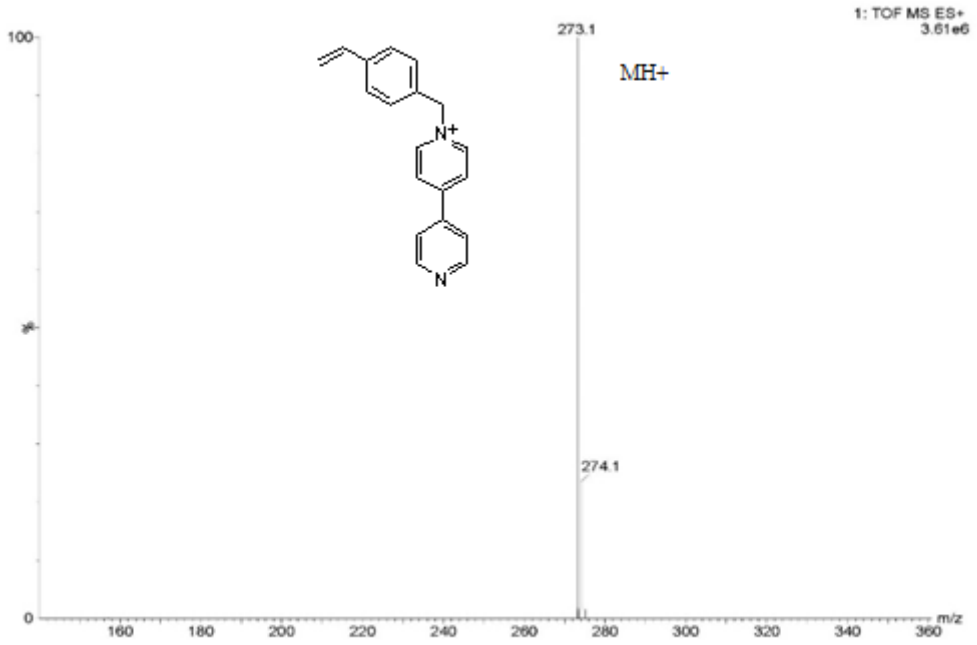

*Figure 14. MS of monomer **1**.*

Figure 13 showed the three peaks corresponding to the vinyl group, *h* (δ 6.7 ppm), *i* (δ 5.3 ppm, trans) and *j* (δ 5.8 ppm, cis). In addition, it was seen that peaks *d* (δ 8.9 ppm) and *c* (δ 8.3 ppm) corresponding to the bipyridine protons were shifted with respect to the peaks *a* (δ 8.7 ppm) and *b* (δ 7.8 ppm) due to the effect of the quaternized nitrogen. These shifts suggest the formation of the monomer **1**.

However, two additional peaks could be seen in the ^{1}H NMR analysis at *a'* 8.4 and *b'* 9.1 ppm that suggested the formation of a side product. Nevertheless, the MS showed only the peak corresponding to 1-(4-vinylbenzyl)-[4,4'-bipyridin]-1-ium cation at 273.1 m/z, which was in agreement with the expected exact mass 273.14 m/z. ^{1}H NMR analysis of pure 4,4'-bipyridine and 4-vinylbenzyl chloride was performed and the existence of residual reagents as well as their impurities in the final product was discarded (^{1}H NMR spectra of both compounds in the Appendix).

Different purification methods such as chromatography column and recrystallization were performed in order to get rid of the impurity. However, the separation of both components was only achieved via HPCL as shown in figure 15. The big peak at retention time 29 min corresponds to monomer **1**, whereas the small peak at retention time 31 min corresponds to the impurity. Nevertheless, since the fraction of the side product collected was too small, it was not possible to characterize it properly.

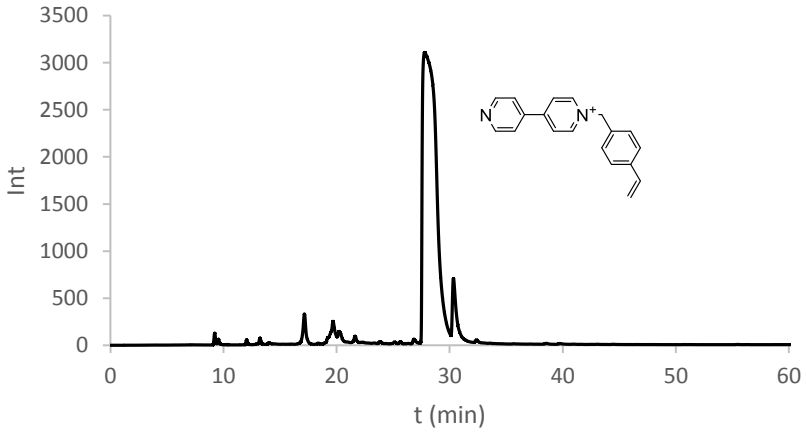

Figure 15. HPLC analysis of the product.

Since the purification to remove this impurity was not achieved, different synthetic conditions were performed in order to study which factors affect the formation of the side product and if it was possible to avoid it.

First, different solvents were used in order to study how the solubility of reagents and product affect the performance of the reaction (Table 6). The solvents were chosen based on two factors. On the one hand, the solubility of the reagents. On the other hand, varying the polarity of the solvents may change the solubility of the monomer **1** and the side product leading to the separation of both compounds by precipitation of one of them. In all the cases shown in table 6, the amount of side product was much higher than those obtained performing the reaction in toluene. Moreover, conversions reached in the experiments 2, 3 and 4 were below 10 % whereas

the experiment 1 yielded a 60% of conversion. The quantification of the side product was done using ^{1}H NMR. All the percentages are given based on the integration of the signals *d* (δ 8.9 ppm) corresponding to monomer **1** and the signal *a'* (δ 9.1 ppm) shown in the figure 13.

It is important take into account that all of the reactions were carried out heating to reflux. All the solvents shown in table 6 have boiling points below the toluene boiling point (111 ^{0}C). Therefore, not only the solubility of the raw materials and products is affecting the reaction, but also the temperature is potentially playing a key role.

*Table 6. Synthesis of monomer **1** in different solvents.*

Experiment	Temperature (^{o}C)	Solvent	Stoichiometry (Bipy:Vinylbenzyl)	Side product (%)	Dielectric constant	Solvents boiling point (^{o}C)
1	Reflux	Toluene	5:1	<7	2.4	111
2	Reflux	THF	5:1	11	7.5	66
3	Reflux	AcOEt	5:1	75	6.0	77
4	Reflux	Hexane	5:1	38	2.0	69

We decided to try different temperatures to study its impact in the final product as shown in table 7. The reaction was carried out at 80 °C since it is a temperature that allows comparison with experiments 2, 3 and 4. In addition, the reaction was performed at 140 °C above the boiling point of the toluene (111 °C) in order to find a trend. The experiment 5 was run in a sealed reactor in order to reach temperatures above the boiling point of the toluene. However, the control over the temperature in this case is poor. It is important to take into account that the boiling point of the mixtures could be higher than the pure solvent for those reactions run at atmospheric pressure.

As shown in table 7, it was observed that the amount of impurities decreased as the temperature increased from 80 ºC to reflux. However, above reflux no improvement was seen since the amount of impurities is similar to that obtained at reflux.

Comparing the experiment 3 discussed previously with the experiment 7, it could be seen that at similar temperatures, the reaction performed in toluene produced 5 times less amount of impurity than the reaction performed in AcOEt. In the case of THF, the amount of side product was the same as in toluene. However, the conversion in THF was below 10% whereas in the case of toluene was 61%.

*Table 7. Synthesis of monomer **1** at different temperatures.*

Experiment	Temperature (ºC)	Solvent	Stoichiometry (Bipy:Vinylbenzyl)	Side product (%)
5	140	Toluene	5:1	4
6	Reflux	Toluene	5:1	2
7	80	Toluene	5:1	11

Therefore, although the temperature plays an important role in the formation of the side product, the solvent has a stronger impact in the performance of the reaction.

The reaction was carried out using different feed stoichiometry. Since the 4,4'-bipyridine is a symmetric molecule with two available positions to react through, it was expected the formation of de double alkylated side product. It is essential to perform the reaction with an excess of bipyridine to avoid the formation of secondary products. Therefore, it was expected that increasing the ratio of bipyridine to a certain point lead to a decrease of the amount of the side product.

Table 8 shows five experiments carried out at different ratios bipy:vinylbenzyl in order to find out what is the impact of the addition of different amounts of 4,4'-bipyridine in the performance of the reaction.

*Table 8. Synthesis of monomer **1** at different 4,4'-bipyridine:4-vinylbenzyl chloride feeding ratios.*

Experiment	Temperature (^{0}C)	Solvent	Stoichiometry (Bipy:Vinylbenzyl)	Side product (%)
8	Reflux	Toluene	0.5:1	46
9	Reflux	Toluene	3:1	3
10	Reflux	Toluene	5:1	2
11	Reflux	Toluene	7:1	2
12	Reflux	Toluene	10:1	6

In particular, experiments 8 and 9 showed the importance of the addition of an excess of bipyridine. Experiment 8 showed that, when there is an excess of vinylbenzyl chloride, the amount of the impurity increases substantially (46%). By contrast, the experiments 9, 10, 11 and 12 performed with and excess of bipyridine showed that the amount of side product decreased significantly. However, it was observed that above the ratio bipy:vinylbenzyl performed in the experiment 8 (3:1), the amount of side product remains in the range of impurities between 2% and 7%. Therefore, increasing the amount of 4,4'-bipyridine above 3:1 did not have positive impact in the reduction of the amount of impurities formed during the reaction.

In order to investigate on the side product, ^{1}H NMR analysis of the monomer **1** at different pH was performed having in mind that the most likely side product is double alkylated bipyridine. The aim of this experiment is to study how displacements of ^{1}H NMR signals of the bipyridine are affected by the pH. These results can be extrapolated and compared with the possible formation of the double alkylated bipyridine.

As figure 16 shows, signals *a, b, c* and *d* shifted to higher ppm as the pH increased due to the protonation of the free pyridine. In the case of the signals *d* and *c* corresponding to the protons of the monoalkylated bipyridine shifts are not as evident as for *a* and *b* corresponding to the protons located in the free pyridine. Assuming that protons *a* and *d* have a similar chemical environment when the free pyridine is protonated, it was observed that as the pH increases, signals *a* and *d* tend to match together with signal *a'* (δ 9.02 ppm) corresponding to the impurity. The same for the signals *b* and *c* that match with signal *b'* (δ 8.45 ppm).

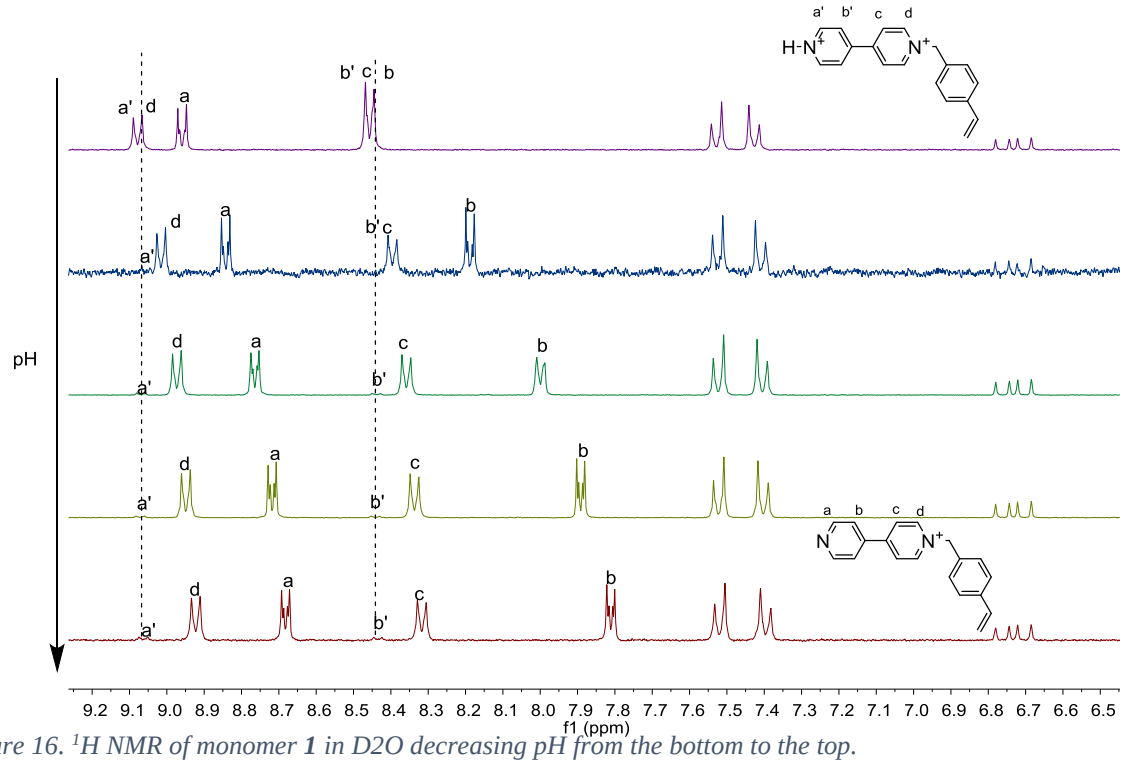

*Figure 16. [1]H NMR of monomer **1** in D2O decreasing pH from the bottom to the top.*

Taking into account the pH experiment with monomer **1**, two possible scenarios arise. On the one hand, the protonation equilibrium of the monomer is slow in ^{1}H NMR time scale. Therefore, the peaks corresponding to both species, protonated and deprotonated can be seen, which is unusual. In addition, it was observed that signals shift when varying the pH proving that the equilibrium is quick in ^{1}H NMR time scale. Therefore, this possibility was discarded.

On the other hand, it was seen that the shifts induced by the protonation of the monomer matched with the potential shifts that the presence of a second quaternized N in the free pyridine ring would induce. Therefore, the most likely scenario was that in which the side product was double alkylated bipyridine.

Assuming that the side product was the double alkylated 4,4'-bipyridine, the integration and comparison of the peak at 8.9 ppm corresponding to product **1**, and the peak at 9.1 ppm corresponding to the impurity were compared in order to calculate the ratio impurities. It indicates that the amount of side product produced in the synthesis was between 2-7% of the total amount of the monomer **1**.

It has to be taken into account that the double alkylated product has two vinyl groups available for polymerization. The main issue that arises from the polymerization of a double alkylated product is the fact that, since two vinyl groups are part of the same molecule, it acts as cross-linker. Therefore, it induced the formation of hyperbranched polymers with poor dispersion control.[32] Nevertheless, taking into account that the percentage of the double alkylated bipyridine in the recipe for the polymerization of the monomer **1** with acrylamide was insignificant (>0.7 % in mole), the degree of cross-linking is expected to be low. Due to time constrains, the effect of the cross-linking in the polymer properties was not studied, which open a window for future work.

After the optimization of the synthesis of the monomer **1**, we decided to perform the reaction at reflux in toluene with a monomer feed stoichiometry of 3:1 (4,4'bipyridine:vinylbenzyl chloride).

Chapter 4

Synthesis and characterization of poly-1-(4-vinylbenzyl)-[4,4'-bipyridin]-1-ium-co-acrylamide

The preparation of the polymer **1** was achieved via free radical polymerization using ACVA as initiator and under oxygen free atmosphere as shown in figure 17. The conditions of the polymerization were obtained from the synthesis of a viologen-polymer reported by U. S. Schubert et al.[33]

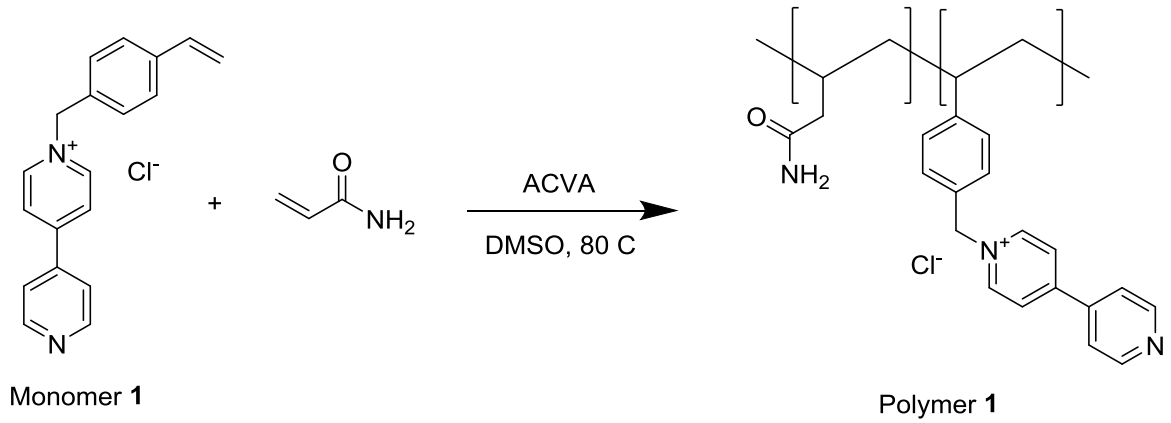

*Figure 17. Scheme of the copolymerization of monomer **1** and acrylamide.*

The ^{1}H NMR on the top of figure 18 showed the spectra corresponding to the crude of the reaction at t = 0, where the signals corresponding to the vinyl groups (5.4 ppm, 5.8 ppm and 6.75 ppm) could be clearly seen. On the other hand, the ^{1}H NMR on the bottom of figure 18 showed the signals corresponding to the final product at the end of the polymerization. It was seen that the signals corresponding to the vinyl groups disappeared. In addition, two broad signals appeared in the aliphatic range indicating the formation of the polymer backbone. It was observed that signals between δ 6.50 ppm and δ 9.50 ppm corresponding to 1-(4-vinylbenzyl)-[4,4'-bipyridin]-1-ium chloride get broader. This broadening in the ^{1}H NMR signals is typical

for polymers and macromolecules because of the loss in the free motion of the structure. Both the apparition of the signals in the range of aliphatic protons and the widening of the signals corresponding to the monomer **1** peaks proved the formation of the polymer.

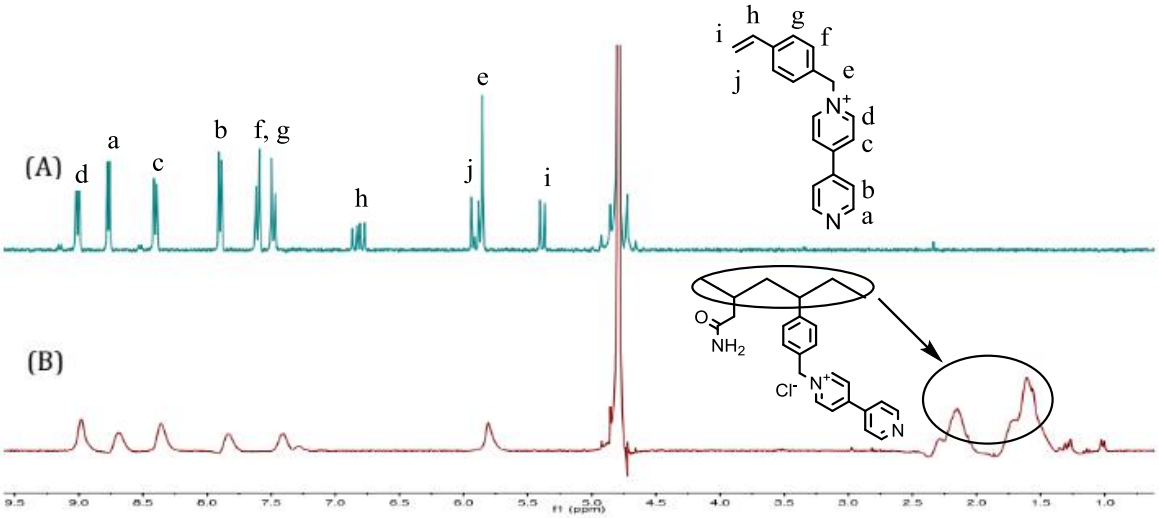

Figure 18. (A) ^{1}H NMR of the polymerization mixture at t = 0 in D_2O. (B) ^{1}H NMR of polymerization mixture at the end of the polymerization in D_2O.

Once the polymerization was demonstrated, primary kinetic experiments indicated a remarkable difference in the conversion of both monomers. As shown in figure 19A and 19B, the consumption of the monomer **1** is faster than the conversion of the acrylamide, especially during the first 60 min of the reaction. As explained in the introduction, the difference in the reactivity ratios can lead to different conformations in the final polymer. Therefore, Kelen-Tüdos method was carried out in order to characterize the reactivity of the monomers in more detail. For this, four reactions were performed (Table 9). The experimental data are shown in table 9 and the values of η and ξ were calculated using equations (4) and (5) explained in the introduction.

$$\eta = \left(r_1 + \frac{r_2}{\alpha}\right)\xi - \frac{r_2}{\alpha} \qquad (4)$$

$$\eta = \frac{G}{\alpha + F}; \qquad \xi = \frac{F}{\alpha + F} \qquad (5)$$

Having in mind that $G=x(1-y)/y$, $F=x^2/y$ and $\alpha = \sqrt{F_m x F_M}$. Being y = (m_1/m_2) and x = (M_1/M_2) the molar ratios of the monomer composition in the polymer and in the feed respectively.

Table 9. Table of calculations for Kelen-Tüdos method.

Experiment	x_{Am}	x_1	y_{Am}	y_1	η	ξ
Poly($M_{0.8}$-Co-$A_{0.2}$)	0.81929	0.1807	0.5115	0.4885	0.6404	0.8216
Poly($M_{0.6}$-Co-$A_{0.4}$)	0.61025	0.3898	0.1968	0.8032	0.2534	0.7012
Poly($M_{0.4}$-Co-$A_{0.6}$)	0.44284	0.5572	0.2045	0.7955	-0.0944	0.3657
Poly($M_{0.2}$-Co-$A_{0.8}$)	0.24534	0.7547	0.1025	0.8975	-0.3704	0.1784

Finally, the calculated parameters were plotted as shown in figure 19C.

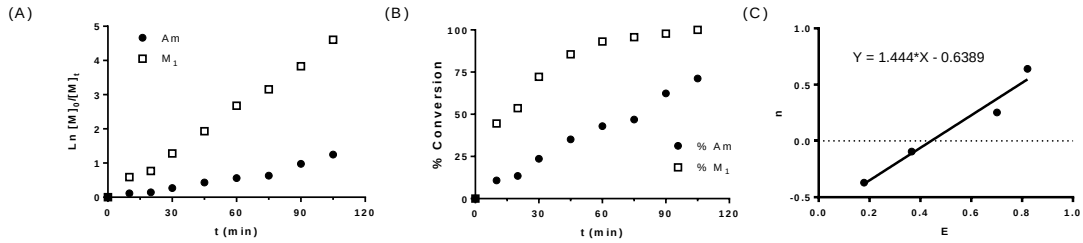

Figure 19. (A)Representative linear plot of $ln[M]_0/[M]_t$ vs time. (B) Conversion of acrylamide and 1-(4-vinylbenzyl)-[4,4'-bipyridin]-1-ium chloride vs time (C) Plot of data obtained via Kelen-Tüdos calculations.

The reactivity ratios were: **r_{Am}= 0.808; r_1= 2.721**. This difference in the reactivity of the monomers indicated that both the monomer **1** and acrylamide react preferably with monomer **1**. These results matched with the primary kinetic experiments that suggested that the monomer **1** reacts faster than acrylamide. Therefore, as discussed in the introduction, the product obtained was a drift polymer with different composition of the polymer chains depending on the time when the chain was formed in the polymerization process. Thus, at the beginning of the reaction, the polymers are rich in monomer **1** whereas as the polymerization evolves, the amount of acrylamide in the polymers increases. However it is important to take into account

that the monomer ratio in the reaction feed is 1:9 (monomer **1**: acrylamide) so the presence of the acrylamide in the polymers formed at the beginning of the polymerization should still be remarkable.

Further characterization of the polymer was performed. The molecular weight (**M_w = 7236 g mol^{-1}**) of the polymer as well as its dispersity in molar mass (**Đ = 3.3**) were obtained through a calibration on GPC using standards. As seen in figure 20, the GPC analysis showed a broad peak at 17 min that corresponds to the polymer **1**. Since the molecular weight distribution was substantially broad, more experiments were performed in order to discard potential issues in the GPC analysis. To this end, GPC analysis of the polyacrylamide made under the same conditions were carried out showing an overlap with the polymer **1** peak. As discussed previously in the kinetic studies, the faster conversion of the monomer **1** might induce the formation of random polymer chains with different compositions. This may cause the bimodal distribution of the peak corresponding to the polymer **1**.

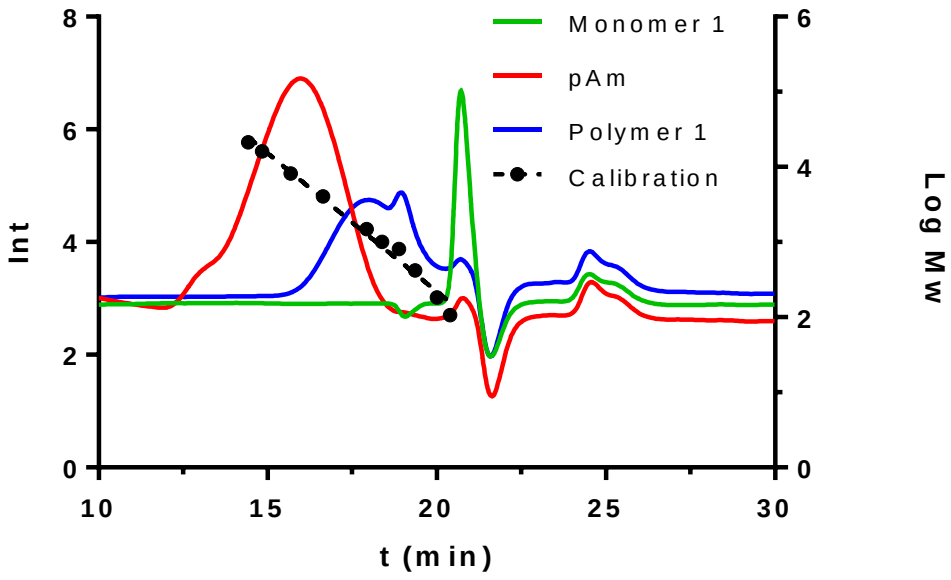

*Figure 20. Comparison of GPC analysis of pure monomer **1**, polyacrylamide and polymer **1**.*

As shown above, the GPC analysis of the polymer **1** showed bimodal distribution so reversible addition-fragmentation chain transfer polymerization experiments were performed in order to try to control the FRP. The RAFT polymerization is a reversible deactivation radical polymerization RDRP,[34] which is a type of controlled radical polymerization. RAFT polymerization was used due to its versatility and easy perform.

The mechanism of the RAFT polymerization is based on the deactivation of growing polymer chains by a control transfer agent to reduce the concentration of active growing chains and minimize termination (Figure 21). In addition, the CTA creates a new radical, which is able to start a new growing chain.[35]

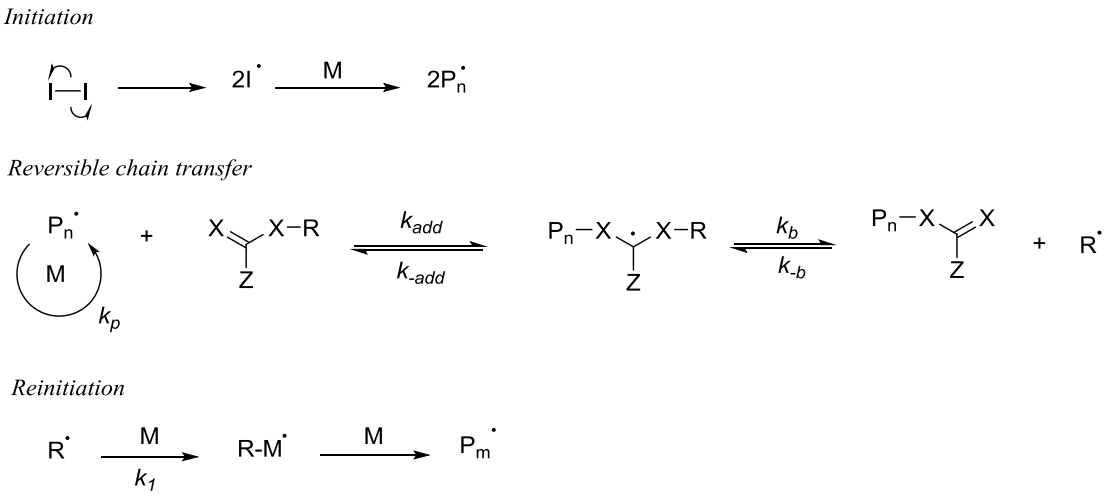

Figure 21. Mechanism of RAFT polymerization.

A CTA, which usually is a thiol derivative, was added directly to the reaction mixture. In this case, the CTA selected was previously used in this group and is shown in figure 22.[36]

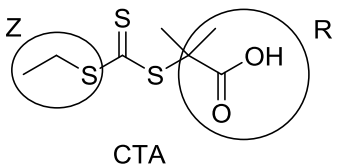

Figure 22. CTA agent used for RAFT polymerization.

Table 10 shows four different experiments in which the ratio initiator:CTA was varied in order

to investigate the effect of the RAFT agent in the system. It was observed that the conversion of both monomers was lower as the amount of CTA increased. This reduction in the conversion of the monomers was more remarkable for the acrylamide that went from 87% of conversion when no CTA was added to a 16% for the polymer **4** where the amount of RAFT agent is the highest. However, since the monomer feed ratio was 9:1 (acrylamide:monomer **1**), all the polymers were mainly composed by acrylamide (>72%).

Table 10. Polymers performed with different amounts of CTA.

Experiment	CTA	T (ºC)	[M]/[CTA]	[CTA]/[In]	[M]/[In]	Bipyridine conversion (%)	Acrylamide conversion (%)	% of bipy in the polymer	% of acrylamide in the polymer
Polymer 1	-	80	-	-	20/1	100	87	10.6	89.4
Polymer 2	Yes	80	100	3/1	300/1	78	48	14.3	85.2
Polymer 3	Yes	80	100	5/1	500/1	77	30	20.7	78.4
Polymer 4	Yes	80	100	9/1	900/1	56	16	26.1	72.4

Figure 23 shows the normalized GPC analysis for the polymers in table 10. It was seen that as the ratio CTA:initiator increased and the conversion of acrylamide decreased, the broad peak disappeared gradually and the narrow peak emerged. In addition, it was observed that the narrow peak corresponding to the copolymer did not change throughout the all experiments. Therefore, it was found that the addition of the CTA did not give control over Đ so the use of RAFT polymerization was discarded.

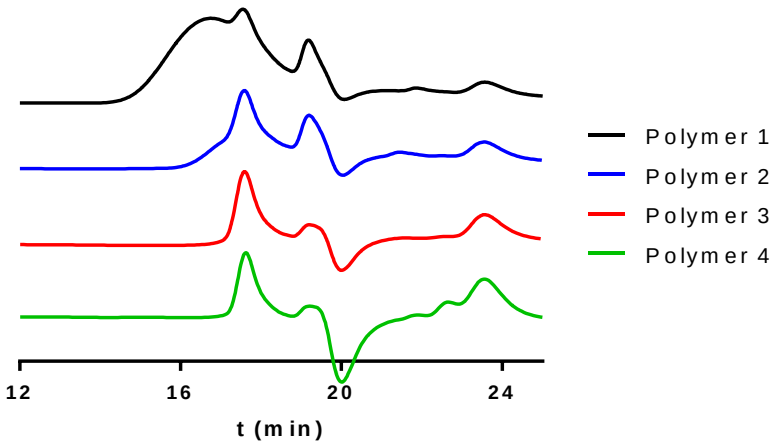

Figure 23. Normalized GPC of polymers synthetized via RAFT polymerization.

Atogether, the synthesis of poly-1-(4-vinylbenzyl)-[4,4'-bipyridin]-1-ium-co-acrylamide was achieved. However, the difference in the reactivity ratios of the acrylamide and the monomer **1** induced a faster conversion of the latter. This lead to the formation of a drift polymer rich in monomer **1** at the beginning of the polymerization. The GPC analysis diplayed a bimodal distribution in the molecular weight. Therefore, the molecular weight and the distribution reported were not reliable. RAFT polymerization was performed. However, no control over the molecular weight and the dispersity was achieved. With this in mind, polymer **1** was chosen for the future experiments.

Chapter 5

Study of the interactions with palladium centres

Having synthetized and characterized polymer **1**, the ability of the polymer to bind Pd(II) centres was studied. First, experiments to prove the complexation of the bis(acetonitrile)palladium(II) (Figure 24) chloride by monomer **1** were performed since it essential to find out whether the monomer is able to bind the palladium salt and study the properties of the complex formed. It is important to take into account that this palladium salt has two labile positions occupied by two acetonitrile ligands. In contrast, the chloride ligands are stable during the all process and stay attached to the palladium center. Figure 25 shows the appearance of two new signals after the addition of 0.4 eq of the Pd(II) complex at *b'* (8.0 ppm) and *a'* (9.1 ppm). Moreover, the intensity of the signals at *b* (7.8 ppm) and *a* (8.75 ppm) corresponding to the protons in the pyridine that can bind the precursor palladium complex decreased.

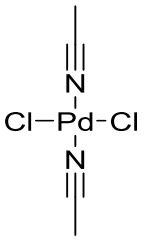

Figure 24. Structure of $[Cl_2(CH_3CN)_2Pd]$

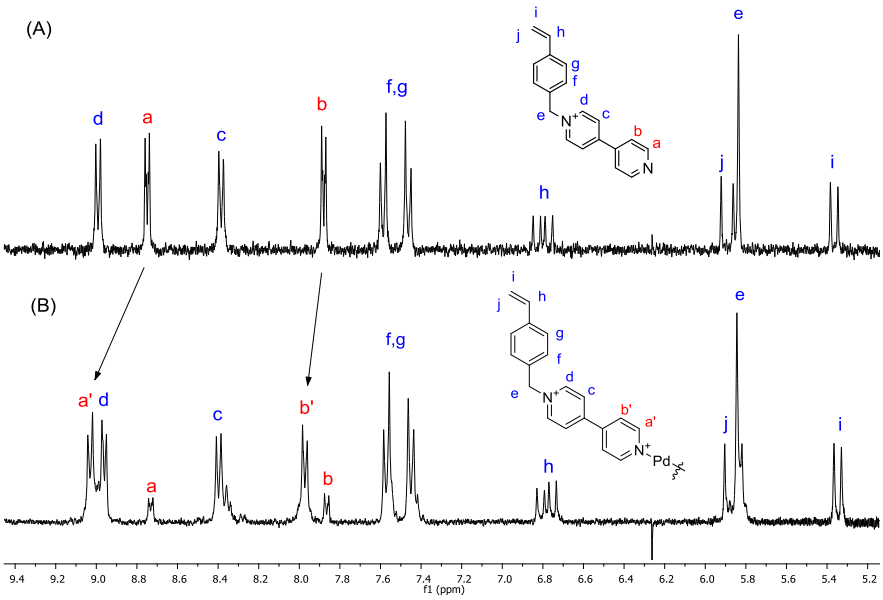

*Figure 25. (A) ^1H NMR of monomer **1** in D_2O. (B) ^1H NMR of monomer **1** after the addition of 0.4 equivalents of bis(acetonitrile)palladium(II) chloride in D_2O.*

Taking into account that the ^{1}H NMR was able to show the signals corresponding to the free monomer as well as the signals corresponding to the monomer binding the metal, the equilibrium between both species is slow in the ^{1}H NMR range time. Otherwise, the ^{1}H NMR spectra would show an average signal shifted from the original position instead of two. This allowed quantifying the amount of complex formed.

UV-Vis analysis was performed in order to confirm results given by ^{1}H NMR experiments. Figure 26 provides data on the UV-Vis experiments after the addition of different amounts of bis(acetonitrile)palladium(II) chloride. The peak at 258 nm corresponds to the absorbance of the 4,4'-bipyridine whereas the shoulder at 300 nm corresponds to the monomer attached to the palladium(II) centre. Since the peak corresponding to the complex formed was overlapping the signal of the monomer, we decided to choose wavelength 300 nm due to the trend that the peak showed as a primary insight of the complex formation. However, further experiments presented then showed that the peak corresponding to the complex formed displayed maxima at 258 nm.

Two different trends could be seen. On the one hand, the signal at 258 nm corresponding to the monomer decreases as the equivalents of the metal complex increases. On the other hand, the signal at 300 nm increased proving that the amount of monomer attached to the metal centre increases suggesting interactions monomer-Pd.

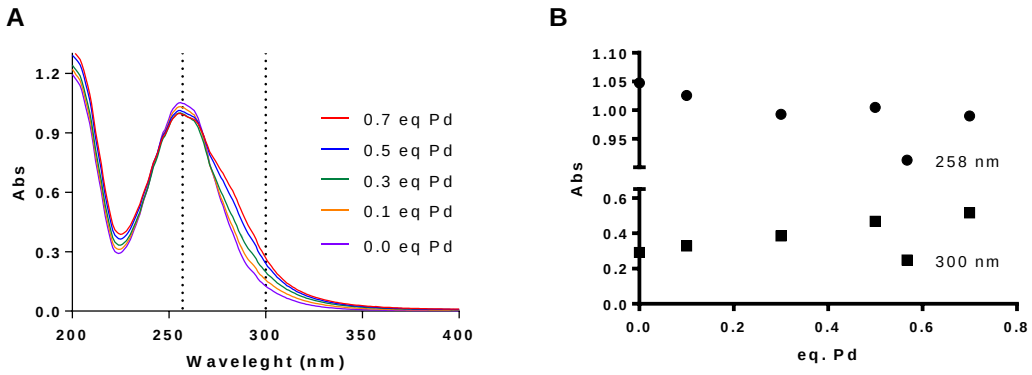

Figure 26. (A) UV-Vis spectra of monomer solution after the addition of different amounts of salt. (B) Absorbance at 258 nm and 300 nm of the samples at different concentrations of palladium salt.

Next, the Job Plot method was performed to have a better understanding of the stoichiometry of the complex formed. The Method of Continuous Variations provides quantitative information on the stoichiometry association as mentioned in the introduction.

First, the ^{1}H NMR experiments for the Job Plot are shown in figure 26. It was seen that as indicated above, the signals corresponding to the studied complex appeared at *b'* (δ 8.0 ppm) and *a'* (δ 9.1 ppm) showing an increasing trend from molar fraction of monomer **1** 0.10 to 0.65 where maxima was reached. However, it was observed that signals *g*, *f* (δ 7.35 ppm), *h* (δ 6.80 ppm), *j* (δ 5.90 ppm), *e* (δ 5.80 ppm) and *i* (δ 5.3 ppm) varied with the molar fraction of the species indicating that the palladium salt interacts not only with the free pyridine, but also with vinyl group.

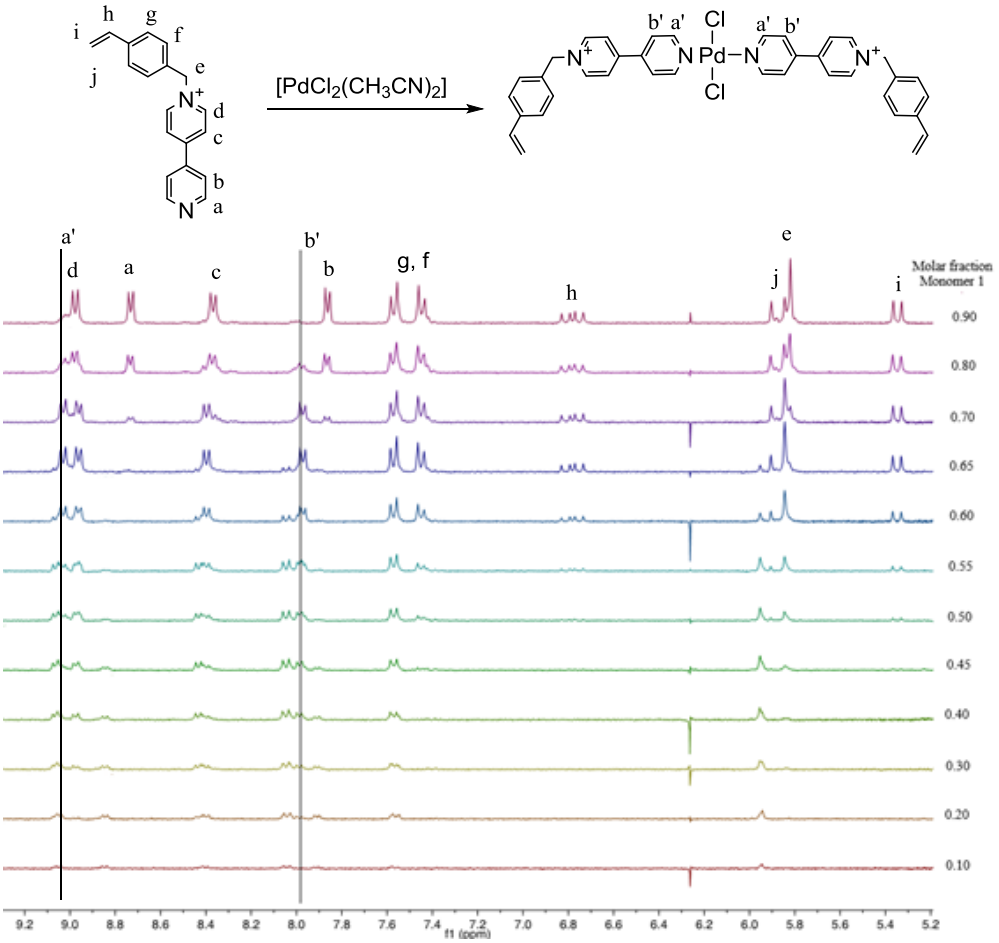

*Figure 27. ^{1}H NMR in D_2O of the monomer **1** after the addition of different equivalents of the palladium salt.*

Results showed that the signals of the vinyl groups were affected only below X_{m1} 0.65 indicating a stronger interaction Pd-pyridine than Pd-vinyl. In addition, it is important to take into account that when the monomer polymerizes the vinyl group disappear. Therefore, there are not potential interferences in the complexation of the palladium salt by the polymer.

On the other hand, UV-Vis experiments for the Job Plot analysis were performed (Figure 28). As mentioned above, the peak corresponding to the monomer **1** overlaps with the peak corresponding to the formed complex (Figure 26A). In order to avoid this interference in the measurements, UV-Vis of each specie was performed separately at same concentrations as samples for Job Plot. Then, the values obtained were subtracted from the spectra performed for the Job Plot samples. As result, a peak at 285 nm corresponding to the absorbance of the formed complex could be seen.

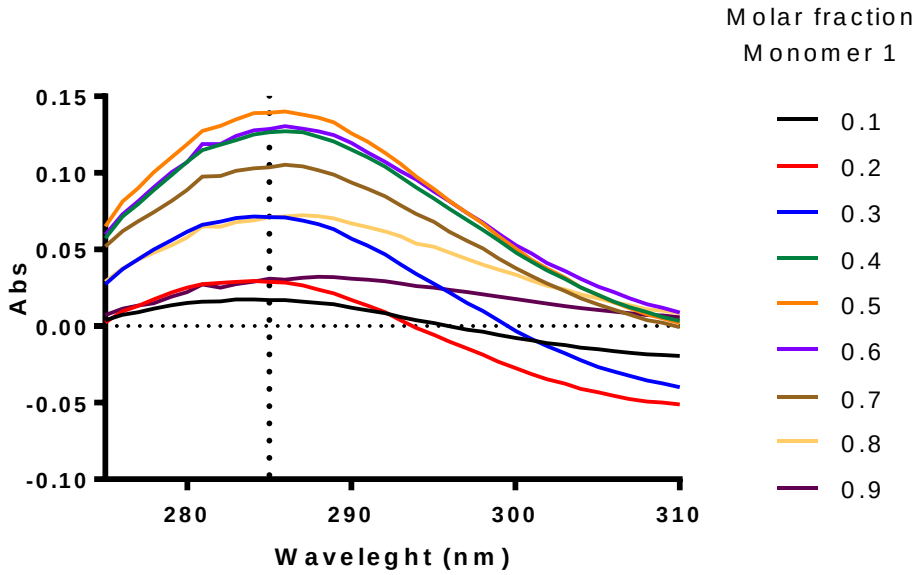

*Figure 52.UV-Vis spectra of samples for the Job Plot experiment after the elimination of potential interferences produced by the monomer **1** and the palladium salt.*

The results from the data obtained from the ^{1}H NMR (Figure 27) were plotted as shown in figure 29B displaying maxima at X_{M1} = 0.65 which indicated that the stoichiometry of the complex formed is 2:1 (monomer **1**:palladium(II)).

On the other hand, results reported by the UV-Vis analysis showed a maximum at $X_{M1} = 0.55$ (Figure 29A). It is important to take into account that although corrections for interferences were done, the signal corresponding to the complex formed overlaps with the signal corresponding to the monomer **1**. This means that the signal corresponding to the complex was affected by the signal of the pyridine, which leads to an error in the values. By contrast, the ^{1}H NMR signals used for the Job Plot in the ^{1}H NMR spectra (*b'* δ 8.0 ppm in figure 27) did not overlap with any other signal so we believe these results are more accurate.

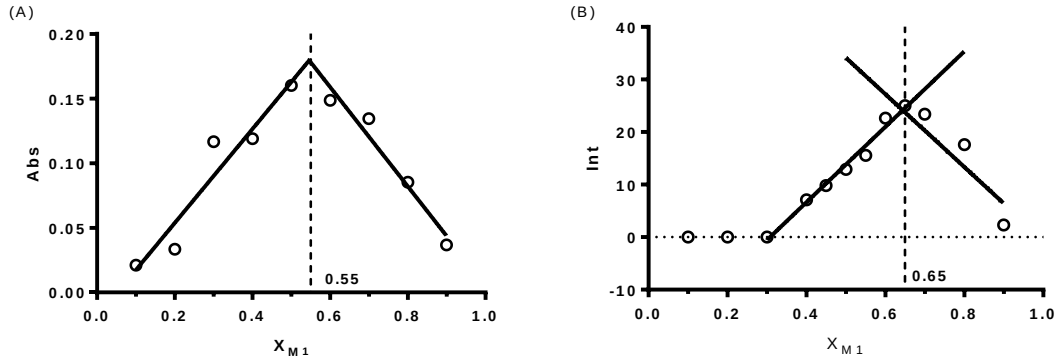

Figure 29. (A) Job Plot from UV-Vis data at wavelength = 300 nm. (B) Job Plot from ^{1}H NMR data at δ 8.0 ppm.

With this in mind, experiments for the polymer complexation were carried out using the ^{1}H NMR spectroscopy. Figure 30 shows how the signals corresponding to the polymer **1** were affected by the addition of $[CH_3CN]_2Cl_2Pd$. The trend indicated that the intensity of the signals decreased with the addition of the palladium salt. It is well known that relaxation time is sensitive to molecular motion. It was expected that the binding of the polymer to palladium lead to a more rigid structure which reduce the free motion of the polymer resulting in a decrease in the intensity of the signals.[37]

These results suggested interactions between the monormer **1** along the polymer **1** and the palladium centers. In addition, it could be seen that after the addition of more than 0.5 eq of the palladium salt, the signals disappeared completely. As described previously, the equivalents of palladium were calculated with respect to the amount of monomer **1** in the polymer **1**.

Considering this, these results were in agreement with the stoichiometry of the formed complex calculated above via Job Plot (2:1).

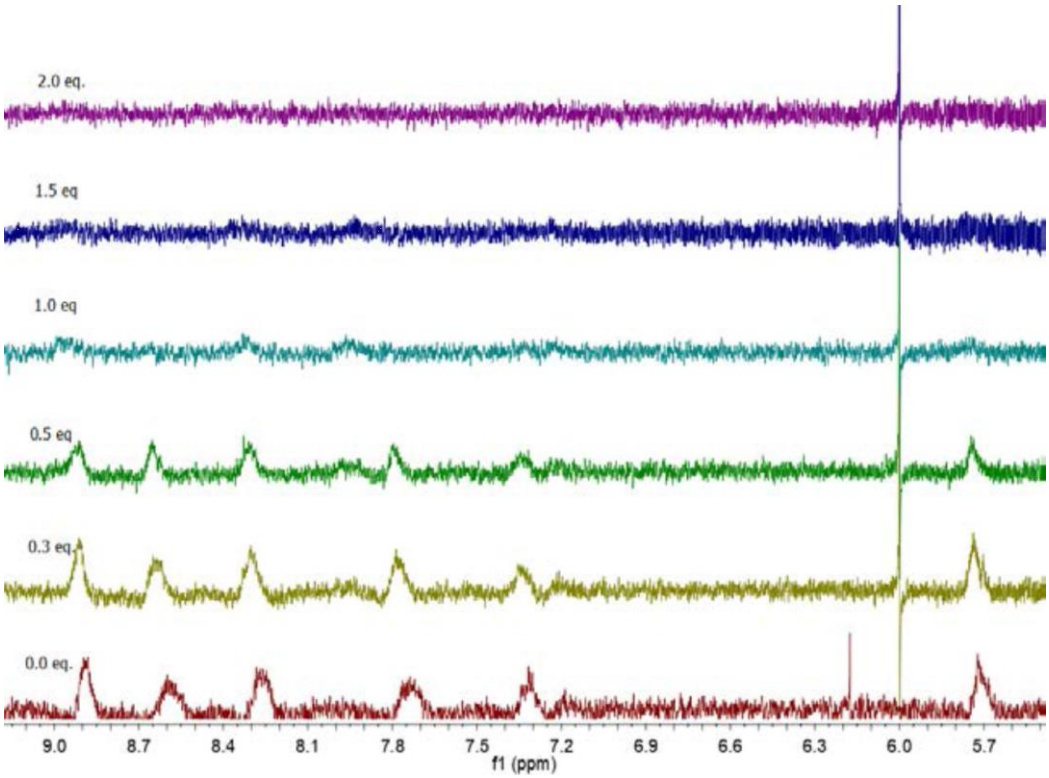

*Figure 30. ^{1}H NMR of polymer **1** after the addition of different equivalents of $[CH_3CN]_2Cl_2Pd$.*

Two different scenarios are possible when the polymer is in solution as shown in figure 31. On the one hand, if the π-π stacking forces are intense enough, the polymer chains aggregate leading in the formation of particles that can be detected by DLS. By contrast, if the π- π stacking forces are not enough to address the aggregation of the polymer, then either no particles are formed so polymer chains move free or the formation of the particles will be addressed by other forces, which make the particles less compact, or polymer chains move free so no particles are formed.

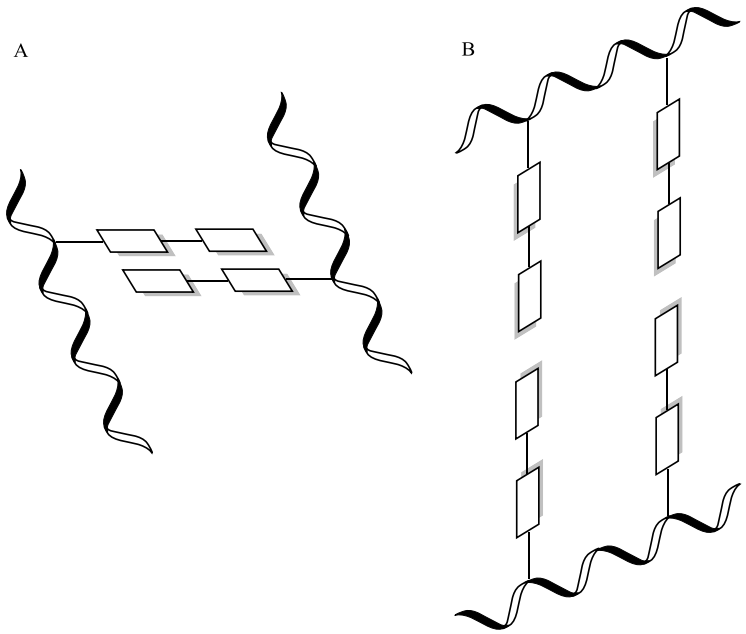

Figure 61. Representation of the two possible scenarios when the polymer is in water. (A) π-π stacking interactions lead to the aggregation of polymer chains forming more compact NP's. (B) No π-π stacking interactions between polymer chains leading in bigger particle sizes.

In the case that polymer chains aggregate directed by π-π stacking forces, then the interaction with the precursor palladium complex will induce the swelling of the particles which leads to the increase of the particle size as shown in figure 32.

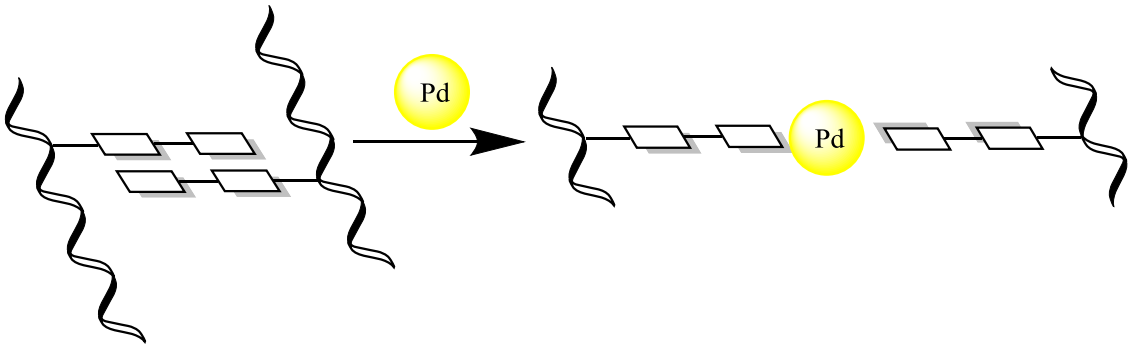

Figure 32. Representation of the polymer particles collapsed by π-π stacking interaction when rearranged after the addition of the precursor palladium complex.

By contrast, in the case that particle collapse driven by non π-π stacking forces, the polymer chains will be far from each other leading in a bigger particle size. When the precursor metal complex is added, the particles will collapse addressed by the palladium centers diminishing their size as shown in figure 33.

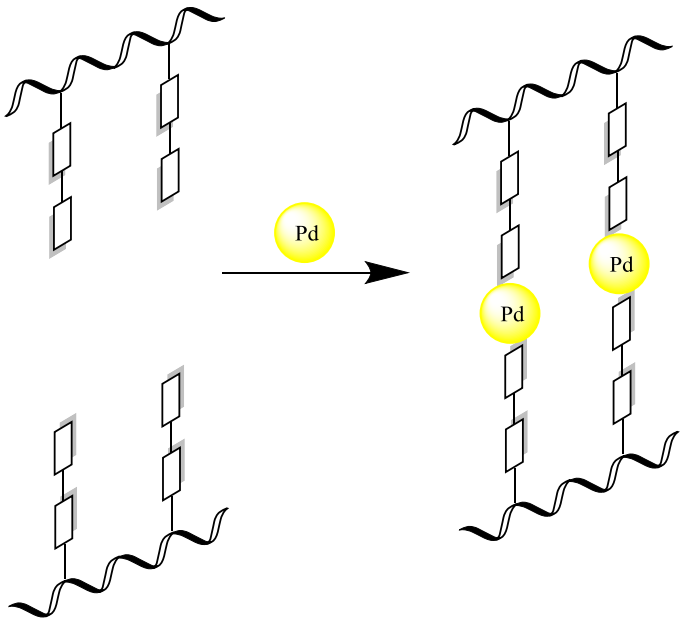

Figure 64. Representation of the polymer particles collapsed by π-π stacking interaction when rearranged after the addition of the precursor palladium complex.

The hydrodynamic diameter of particles could be determined by (DLS). Therefore, by analysing the size of the particles, it could be seen whether the addition of palladium(II) complex to a polymer solution induced a change in the particle size which indicated an interaction between both species.

With this in mind, DLS experiments were carried out in order to have a better insight of the polymer in solution as well as the effect of the addition of palladium centers. First, results indicated that when no $[CH_3CN]_2Cl_2Pd$ was added, the DLS displays particle sizes between 125 nm and 140 nm as shown in figure 34. This proved that the polymer form aggregates in solution as discussed previously. Then, when the precursor palladium complex was added to the polymer solution, the three graphs show the same increasing size trend in the particle size proving that the polymer interacted with the palladium centers, which was in agreement with results presented previously. As discussed above, this increase in the particle size indicated that polymer particles in solution aggregate directed by π-π stacking interactions, which makes

particles compact, and when the precursor palladium complex was added, the polymer chains rearranged directed by the interactions polymer-Pd making the particles swell.

An increasing trend was seen in the three different experiments carried out at different polymer concentrations. However, the effect varied depending on the concentration. For particles made at 0.5 $mgmL^{-1}$ polymer solution, there was a slight change in the size of the particles whereas in the case of 2.0 $mgmL^{-1}$ the increment was significantly higher. Therefore, the increment in the particle size addressed by the addition of the metal was more prominent when the concentration of the species is higher proving that the conformation of the particles depends on the concentration of the species. This may have a huge impact according to the potential applications such as in catalysis which lead to a potential future work.

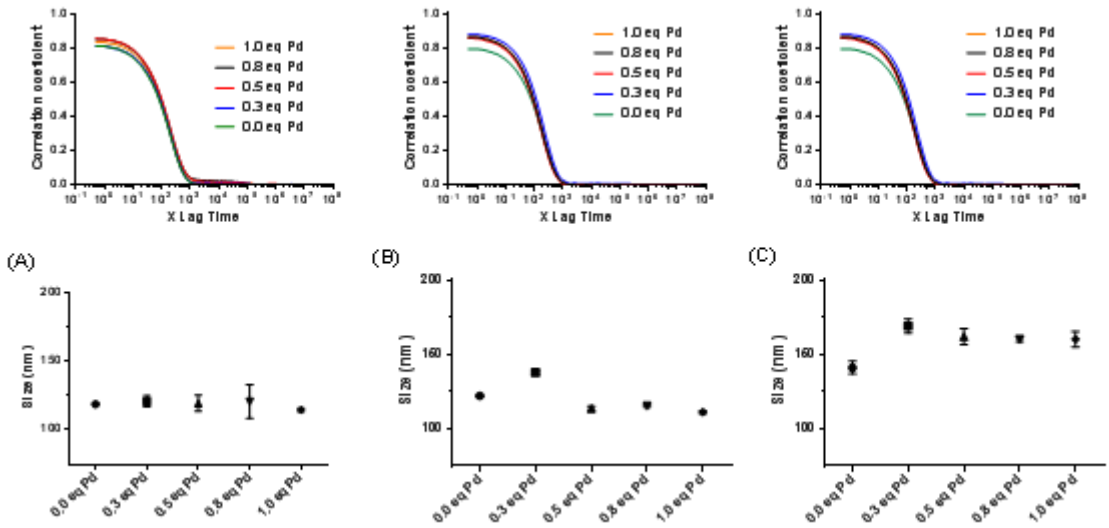

Figure 34. DLS results for the study of the impact of in particle size when adding palladium complex to a polymer solution. (a) 0.5 $mgmL^{-1}$ of polymer 1. (b) 1.0 $mgmL^{-1}$ of polymer 1. (c) 2.0 $mgmL^{-1}$ of polymer 1.

Moreover, it was found that after the addition of 0.3 equivalents of $[CH_3CN]_2Cl_2Pd$, further addition of the metal leads to a gentle decrease in the particle size. Furthermore, above 0.5 equivalents of palladium no substantial change is observed, which was in agreement with the results obtained in the Job Plot experiment that indicated a 2:1 (monomer:palladium) stoichiometry.

Chapter 6

Conclusions

The synthesis of 1-(4-vinylbenzyl)-[4,4'-bipyridin]-1-ium chloride was achieved. Nevertheless, the formation of a side product was observed. Two different strategies were performed in order to minimize the amount of impurity formed during the reaction. Three purification methods were tried. Recrystallization and chromatography column were not able to separate both compounds. By contrast, HPLC was able to separate both compounds but it was not possible to collect a pure fraction of the secondary product.

Since the purification was not possible, the synthesis of monomer **1** was performed under different conditions in order to minimize the amount of the impurity. It was shown that the solvent plays a key role being toluene the solvent that provided the best results. The impact of the temperature was studied. It was found that as the temperature tend to the reflux, the amount of the secondary product diminishes. However, no improvement was observed above the temperature of reflux. Finally, different ratios of reagents in the feed were performed proving the need of using an excess of 4,4'-bipyridine in the feed. It was demonstrated that the optimum feed ratio was of 3:1.

The polymerization of the monomer **1** together with acrylamide was achieved via FRP. The kinetic studies showed a remarkable difference between the reactivity of both monomers. The reactivity ratios of the monomers were obtained via Kelen-Tüdos method. It was found that for the monomer **1** the reactivity ratio was $\mathbf{r_1 = 2.7209}$ whereas in the case of the acrylamide $\mathbf{r_{Am} = 0.8075}$. This difference in reactivity ratio indicated that random polymers were obtained. However, the ratio monomer **1**:acrylamide along the polymer chains varied as the

polymerization reaction went on. Polymers formed at the beginning of the reactions were richer in monomer **1** than those formed at the end. GPC analysis showed a bimodal distribution

RAFT polymerization was performed in order to try to control the polymerization process. It was found that the addition of a CTA agent diminished the conversion of the monomers. In addition, GPC analysis showed that the addition of the RAFT agent did not give any control over the molar mass of the polymers obtained. Therefore, we decided to carry on with the polymers synthetized via FRP.

On the other hand, it was found that the monomer interacts with the palladium forming a new complex. The Job Plot method indicated that the stoichiometry of the complex formed was 2:1 (monomer 1:palladium(II)). ^{1}H NMR experiments of the polymer **1** together with palladium salts were performed suggesting that monomer **1** interacts when it is in the polymer. Further experiments with DLS showed that the addition of palladium(II) to a polymer solution induced a change in the particles size. It has been found that the size of the particles increases due to the self-assembly of the polymer driven by the addition of $[CH_3CN]_2Cl_2Pd$, which suggested the interaction between the polymer 1 and the palladium centers and therefore, the formation or the Pd-NP's.

Altogether, it was proved that the polymer 1 is able to bind palladium(II) complex and form palladium(II) metalorganic nanoparticles in solution.

Chapter 7

Future work

The work presented herein suggested the formation of the nanoparticles made of polymer 1 directed by palladium(II) centers. However, some issues arises. As mentioned in the introduction, one of the potential applications is using these Pd-NP's as catalyst for C-C coupling reactions in water. Therefore, investigation of the ability Pd-NP's to catalyse these reactions becomes a potential later work.

As indicated in chapter 3, the existence of the double alkylated bipyridine impurity can lead to the formation of a hyperbranched polymers. This may affect not only properties of the polymer such as solubility, but also its performance when interacting with palladium centers. Thus, the study of the polymer conformation becomes a potential future work.

In addition, one of the advantages of similar systems is that NP's can be recovered from the reaction crude to reuse them in further reactions. For this, the stability of the particles and their ability to not degrade loosing palladium and for hence catalytic activity must be studied.

Appendix

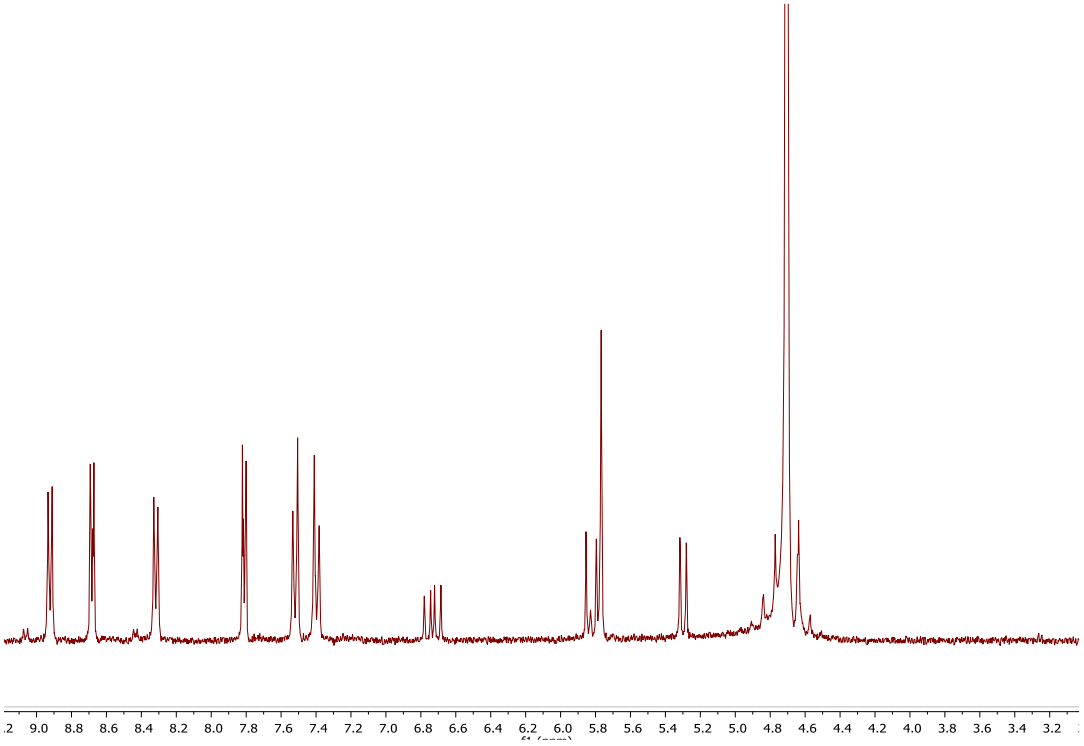

*Figure 35. ^{1}H NMR of monomer **1** in D_2O.*

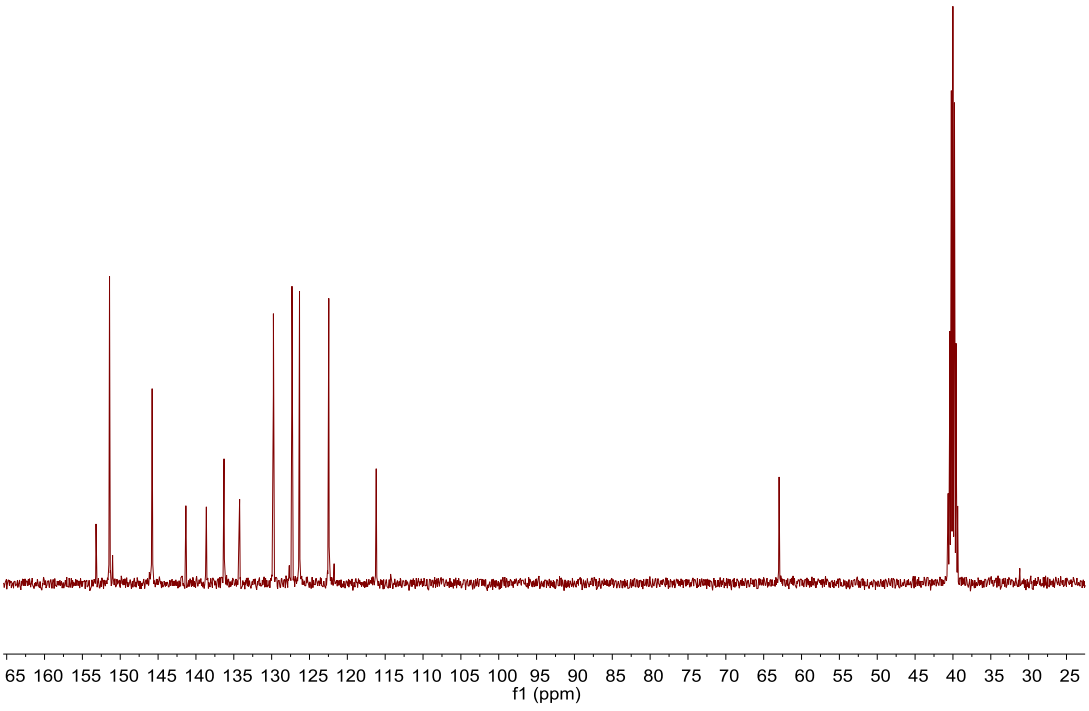

*Figure 36. ^{13}C NMR of monomer **1** in D_2O.*

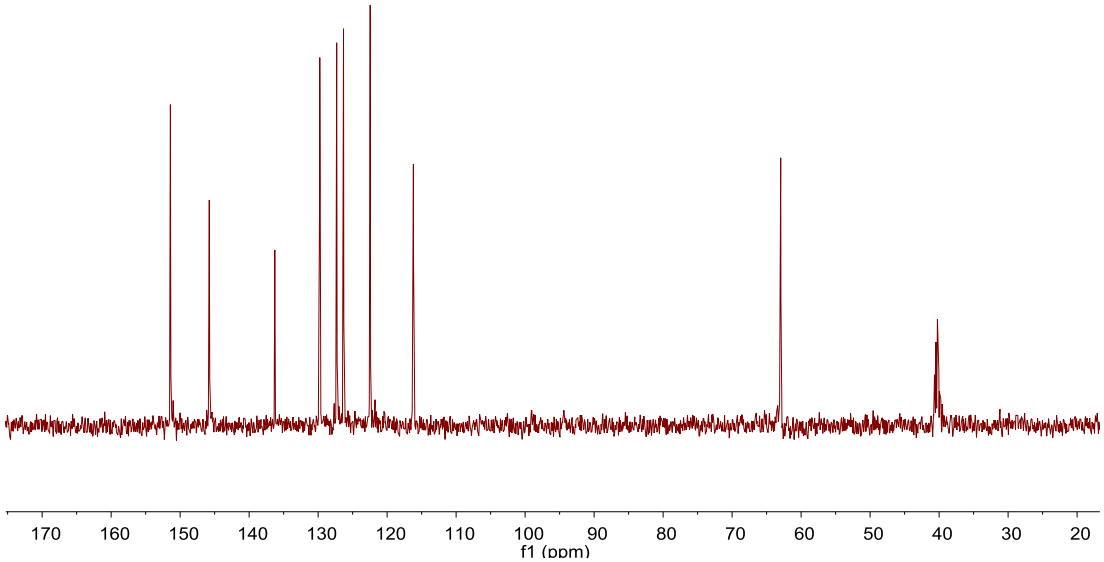

*Figure 37. DEPT of the monomer **1** in D_2O.*

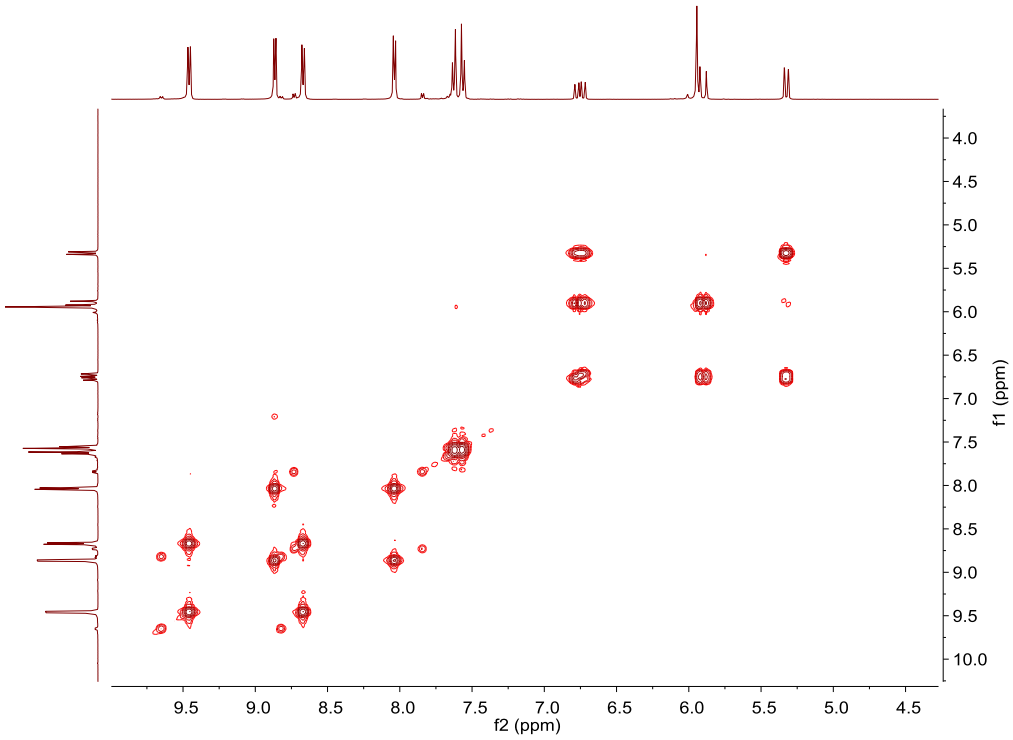

*Figure 38. COSY of monomer **1** in D_2O.*

Appendix

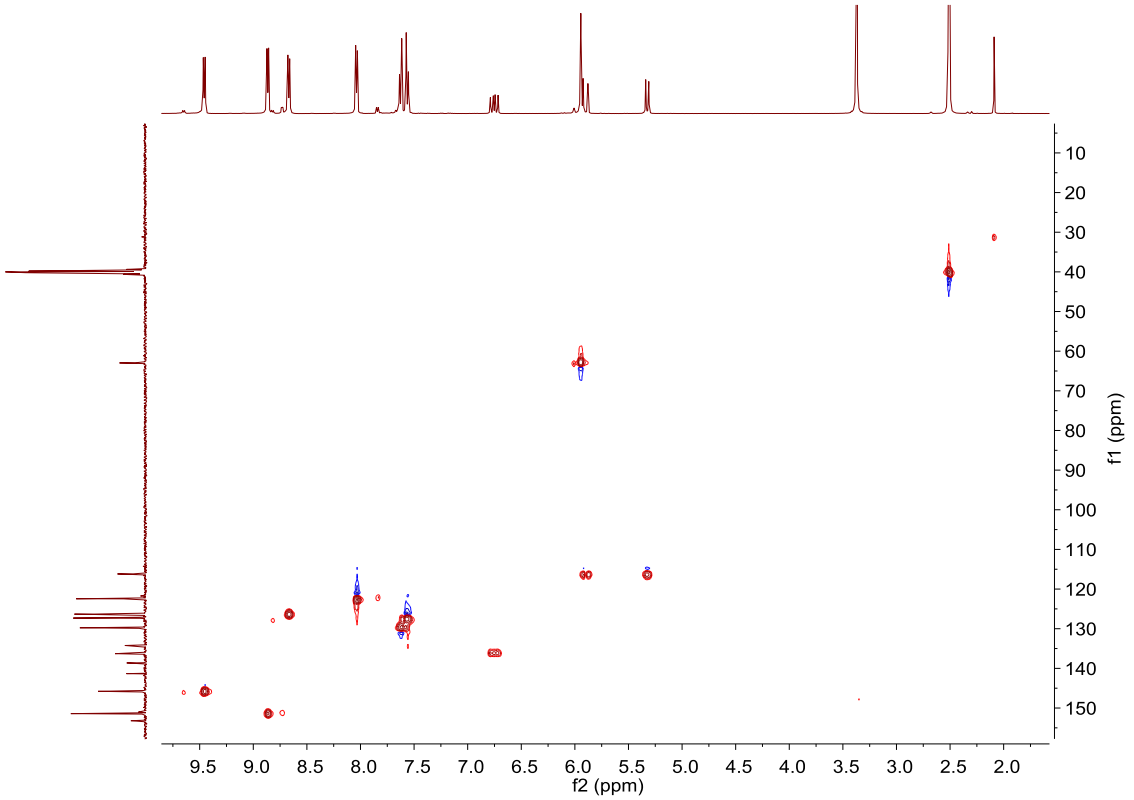

*Figure 39. HSQC of monomer **1** in D_2O.*

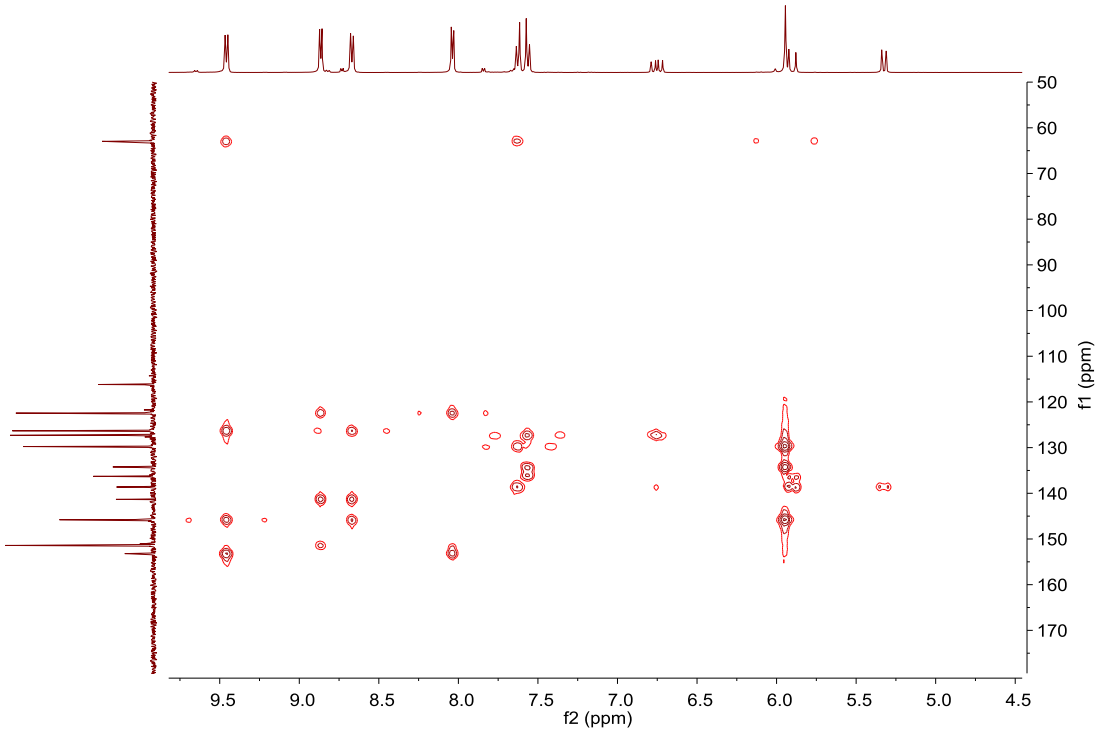

*Figure 40. HMBC of monomer **1** in D_2O*

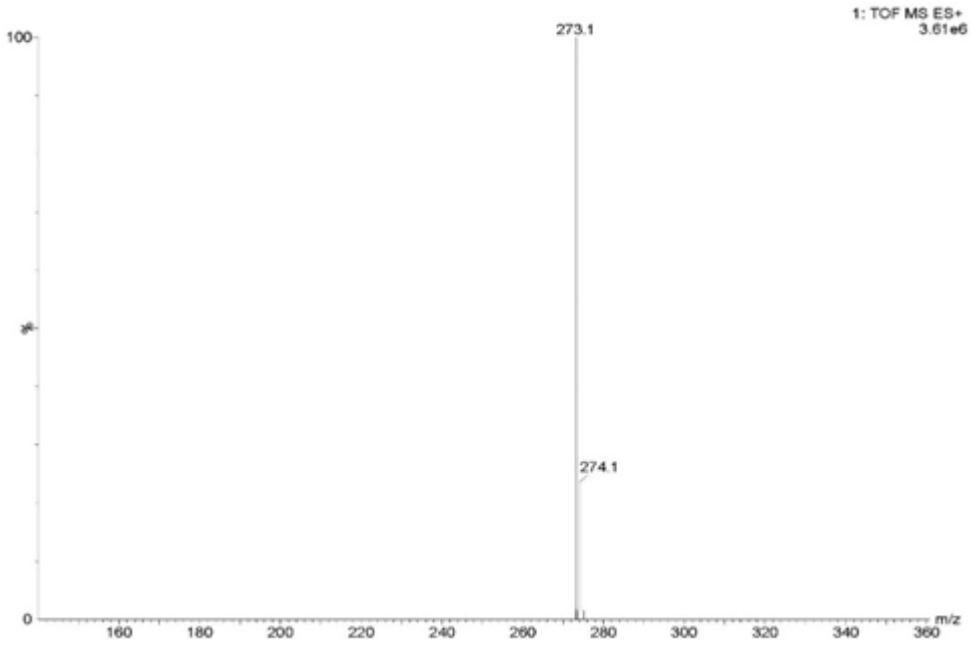

*Figure 41. Mass spectra of monomer **1**.*

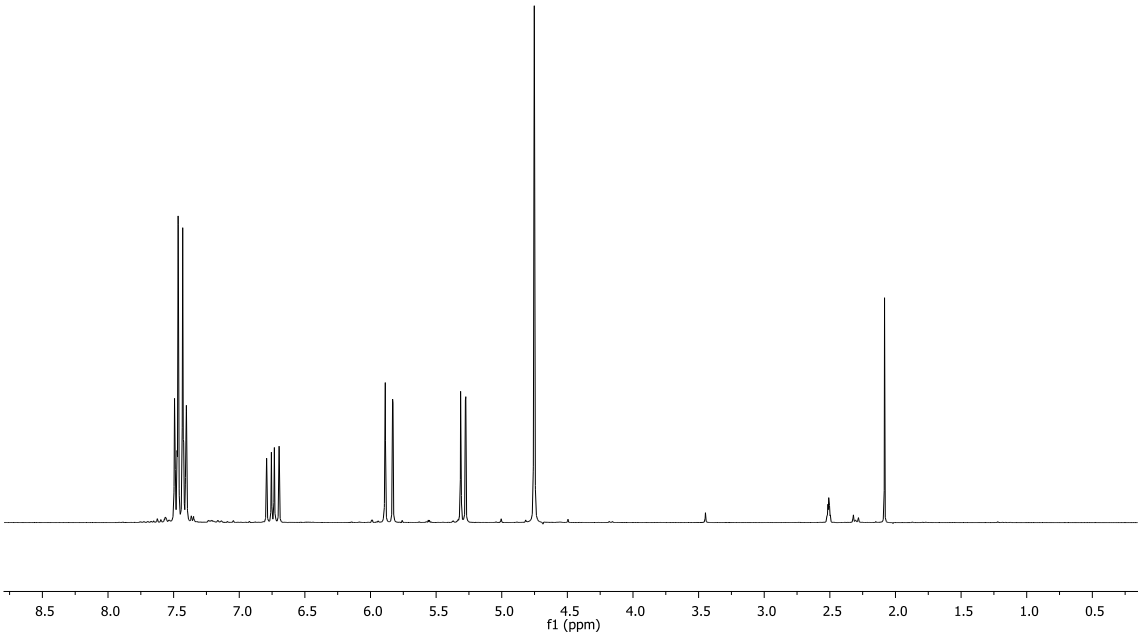

Figure 42. ^{1}H NMR of 4-vinylbenzyl chloride in D_2O.

Appendix

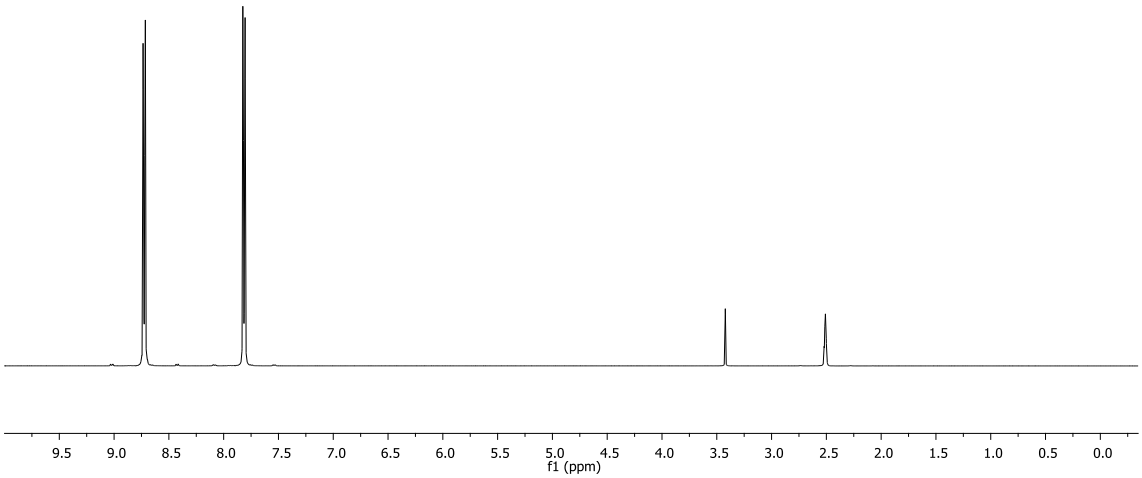

Figure 43. ^{1}H NMR of 4,4-bipyiridine in DMSO-d_6.

Bibliography

[1] C. C. Johansson Seechurn, M. O. Kitching, T. J. Colacot, V. Snieckus,. *Angew. Chem. Int. Ed.* 2012, 51, 5062–5085.

[2] (a) K. H. Shaughnessy, R. B. De Vasher,. *Org. Chem.* 2005, 9, 585–604.

(b) Aqueous-Phase Organometallic Catalysis, eds. B. Cornils, W. A. Herrmann, Wiley-VCH, Weinheim, 2nd ed, 2004.

(c) A. Lubineau, In Modern Solvents in Organic Synthesis, ed. P. Knochel, Springer, Berlin, 1999.

(d) Organic Synthesis in Water, ed. P. A. Grieco, Blackie Academic & Profesional, London, 1998.

(e) Aqueous- Phase Organometallic Catalysis, Concepts and Applications, eds. B. Cornils, W. A. Herrmann, Wiley-VCH, Weinheim, 1998.

(f) C.-J. Li, T.-H. Chen, Organic Reactions in Aqueous Media, Dordrecht, 1997.

[3] (a) F. Joo, Aqueous Organometallic Catalysts, Kluwer, Dordrecht, 2001.

(b) R. Breslow,. *Acc. Chem. Res.* 1991, 24, 159-164.

(c) L. C. Jun,. *Chem. Rev.* 1993, 93, 2023-2035.

[4] (a) N. E. Leadbeater, M. Marco,. *Chem. Rev.* 2002, 102, 10, 3217-3274.

[5] (a) L.-C. Lee, J. He, J.-Q. Yu, C. W. Jones,. *ACS Catal.* 2016, 6, 5245-5250.

(b) J. Gil-Moltó, S. Karlström, C. Nájera,. *Tetrahedron*, 2005, 61, 12168-12176.

[6] G. R. Newkome, V. K. Gupta, F. R. Fronczek,. *Organometallics*, 1982, 1, 907-910.

Bibliography

[7] G. P. F. Van Strijdonck, M. D. K. Boele, P. C. J.Kamer, J. G. de Vries, P. W. N. M. van Leeuwen,. *Eur. J. Inorg. Chem.* 1999, 7, 1073-1076.

[8] R. M. Buchmeiser, K. Wurst,. *JACS*, 1999, 121, 11101-11107.

[9] (a) N. A. Bumagin,. *Cat. Com.* 2016, 79, 17–20.

(b) E. Buxaderas, D. A. Alonso, C. Najera,. *Eur. J. Org. Chem*. 2013, 26, 5864–5870.

[10] J. A. Gladysz,. *Chem. Rev.* 2002, 102, 3215-3216.

[11] N. D. Knöfel, H. Rothfuss, J. Willenbacher, C. Barner-Kowollik, P. W.Roesky,. *Angew Chem Int Ed Engl.* 2017, 56, 4950-4954.

[12] J. Willenbacher, O. Altintas, V. Trouillet, N. Knöfel, M. J. Monteiro, P. W. Roesky, C. Barner-Kowollik,. *Polym. Chem.* 2015, 6, 4358-4365.

[13] I. Berkovich, S. Mavila, O. Iliashevsky, S. Kozuch, N. G. Lemcoff,. *Chem. Sci.*, 2016, 7, 1773-1778.

[14] A. Sanchez-Sanchez, A. Arbe, J. Colmenero, J. A. Pomposo,. *ACS Macro Letters*, 2014, 3, 439–443.

[15] (a) M. Kryszewski,. *Polym. Adv. Tech*. 1998, 9, 224–259.

(b) I. Muzammil, Y. Li, M. Lei, *Plasma Processes and Polymers*. 2017, 14, 1700053.

(c) U. Beginn, *Colloid Polym. Sci*. 2008, 286, 1465–1474.

(d) K. Matyjaszewski, J. Z. Michael, V. A. Stephen, G. Dorota, P. Tadeusz,. *J. Phys. Org. Chem*. 2000, 13, 775–786.

[16] K. S. Rajdeo, S. Ponrathnam, S. Pardeshi, N. N. Chavan, S. S. Bhongale, R. Harikrishna.. *J. Macromo. Sci.* 2015, 52, 982–991.

[17] F. R. Mayo, F. M. Lewis,. *J. Am. Chem. Soc.* 1944, 66, 1594–1601.

[18] M. Fineman, S. D. Ross,. *J. Polym. Sci.* 1950, 5, 259–262.

[19] (a) M. Kucharski, A. Ryttel,. *Polymer*, 1984, 25, 555-558.

(b) T. Kelen, F. Tüdös, B. Turcsányi,. *Polymer Bulletin.* 1980, 2, 71-76.

[20] S. Jindabot, K. Teerachanan, P. Thongkam, S. Kiatisevi, T. Khamnaen, P. Phiriyawirut, S. Charoenchaidet, T. Sooksimuang, P. Kongsaeree, P. Sangtrirutnugul,. *J. Organomet. Chem*. 2014, 750, 35-40.

[21] (a) K. L. Billingsley, K. W. Anderson, S. L. Buchwald *Angew. Chem. Int. Ed*. 2006, 45, 3484-3488.

(b) C. A. Fleckenstein, H. Plenio, *Chem. Eur. J*., 2007, 13, 2701-2716.

[22] G. Altenhoff, R. Goddard, C.W. Lehmann, F. Glorius,. *Angew. Chem. Int.* 2003, 42, 3690-3693.

[23] (a) D.-H. Lee, M.-J. Jin,. *Org. Lett*. 2011, 13, 252-255.

(b) J. S. Renny, L. L. Tomasevich, E. H. Tallmadge, D. B. Collum,. *Angew. Chem. Int.* 2013, 52, 11998–12013.

[24] I.D. Kostas, A.G. Coutsolelos, G. Charalambidis, A. Skondra, *Tetrahedron Lett*., 2007, 48, 6688-6691.

[25] (a) E. Amadio, M. Bertoldini, A. Scrivanti, G. Chessa, V. Beghetto, U. Matteoli, R. Bertani, A. Dolmella,. *Inorg. Chim*. 2011, 370, 388-393.

(b) L. Shen, S. Huang, Y. Nie, F. Lei,. *Molecules*, 2013, 18, 1602-1612.

[26] N. Shahnaz, B. Banik, P. Das, *Tetrahedron Lett*., 2013, 54, 2886-2889.

[27] (a) T. Weilandt, N. L. Löw, G. Schnakenburg, J. Daniels, M. Nieger, C. A. Schalley, A. Lützen,. *Chem. Eur. J.* 2012, 18, 16665-16676.

(b) F. R. Hartley,. *Coord. Chem. Rev.* 1981, 35, 143.

(c) S. L. Jeon, D. M. Loveless, W. C. Yount, S. L. Craig,. *Inor. Chem.* 2006, 45, 11060-11068.

[28] M. Fujita, J. Yazaki, K. J. Ogura,. *Am. Chem. Soc*. 1990, 112, 5645-5647.

Bibliography

[29] (a) T. Rama, C. Alvariño, O. Domarco, C. Platas-Iglesias, V. Blanco, M. D. García, C. Peinador, J. M. Quintela, *Inorg. Chem*. 2016, 55, 2290-2298.

(b) S. R. Seidel, P. J. Stang, *Chem. Res.* 2002, 35, 972-983.

(c) E. Zangrando, M. Casanova, E. Alessio,. *Chem. Rev*. 2008, 108, 4979-5013.

[30] P. Job,. *Ann. Chim*. 1928, 9, 113–203.

[31] J. S. Renny, L. L. Tomasevich, E. H. Tallmadge, D. B. Collum,. *Angew. Chem.* 2013, 52, 11998–12013.

[32] R. M. England, S. Rimmer,. *Polym. Chem*. 2010, 10, 1533–1544.

[33] T. Janoschka, S. Morgenstern, H. Hiller, C. Friebe, K. Wolkersdörfer, B. Häupler, M. D. Hager, U. S. Schubert,. *Polym. Chem.* 2015, 45, 7801-7811.

[34] A. D. Jenkins, R. G. Jones, G. Moad,. *Pure Appl. Chem*. 2009, 82, 483−491.

[35] G. Moad, E. Rizzardo, S.H. Thang,. *Aust. J. Chem*. 2012, 65, 985–1076.

[36] G. Yaşayan, M. Redhead, J. P. Magnusson, S. G. Spain, S. Allen, M. Davies , C. Alexander, F. Fernandez-Trillo,. *Polym. Chem.* 2012, 3, 2596-2604.

[37] (a) G. Njikang, I. Kwan, G. Wu, G. J. Liu,. *Polymer*, 2009, 50, 5262–5267.

(b) F. Cau, S. Lacelle,. *Macromolecules*, 1996, 29, 170–178.